Effects of gold nanoparticles in gilthead seabream – a proteomic approach

A. Barreto[1*], A. Carvalho[1], A. Campos[2], H. Osório[3,4,5], E. Pinto[6], A. Almeida[6], T. Trindade[7], A.M.V.M. Soares[1], K. Hylland[8], S. Loureiro[1], M. Oliveira[1]

[1] Departamento de Biologia & CESAM, Universidade de Aveiro, 3810-193 Aveiro, Portugal

[2] CIIMAR, Centro Interdisciplinar de Investigação Marinha e Ambiental, Universidade do Porto, 4450-208 Matosinhos, Portugal

[3] i3S – Instituto de Investigação e Inovação em Saúde, Universidade do Porto, Porto, Portugal

[4] Instituto de Patologia e Imunologia Molecular da Universidade do Porto, IPATIMUP, Porto, Portugal

[5] Faculdade de Medicina, Universidade do Porto, Portugal

[6] LAQV-REQUIMTE, Departamento de Ciências Químicas, Faculdade de Farmácia, Universidade do Porto, Rua Jorge Viterbo Ferreira, 228, 4050-313 Porto, Portugal

[7] Departamento de Química & CICECO - Aveiro Instituto de Materiais, Universidade de Aveiro, 3810-193 Aveiro, Portugal

[8] Department of Biosciences, University of Oslo, PO Box 1066, N-0316 Oslo, Norway

*Corresponding author: E-mail: abarreto@ua.pt, Tel +351 234 370 350, Fax +351 234 372 587

Highlights

- Gold nanoparticles (AuNPs) induced proteomic changes in *Sparus aurata* liver;
- A total of 26 proteins exhibited differences in abundance;
- The alterations were dependent on the nanoparticles' characteristics;
- AuNPs triggered pathways related to different metabolic processes.

Abstract

Despite the widespread use of nanoparticles (NPs), there are still major gaps of knowledge regarding the impact of nanomaterials in the environment and aquatic animals. The present work aimed to study the effects of 7 and 40 nm gold nanoparticles (AuNPs) – citrate and polyvinylpyrrolidone (PVP) coated – on the liver proteome of the estuarine/marine fish gilthead seabream (*Sparus aurata*). After 96 h, exposure to AuNP elicited alterations on the abundance of 26 proteins, when compared to the control group. AuNPs differentially affected several metabolic pathways in *S. aurata* liver cells. Among the affected proteins were those related to cytoskeleton and cell structure, gluconeogenesis, amino acids metabolism and several processes related to protein activity (protein synthesis, catabolism, folding and transport). The increased abundance of proteins associated with energy metabolism (ATP synthase subunit beta), stress response (94 kDa glucose-regulated protein) and cytoskeleton structure (actins and tubulins) may represent the first signs of cellular oxidative stress induced by AuNPs. Although higher gold accumulation was found in the liver of *S. aurata* exposed to 7 nm PVP-AuNPs, the 7 nm cAuNPs were more bioactive, inducing more effects in liver proteome. Gold accumulated more in the spleen than in the other assessed tissues of *S. aurata* exposed to AuNPs, highlighting its potential role on the elimination of these NPs.

Keywords: nanoparticles, *Sparus aurata*, liver, 2-DE, proteomics

1. Introduction

Despite the many applications of nanotechnology in products of daily use, there are still major gaps in our knowledge regarding the impact of nanomaterials to biota (Matysiak et al. 2016). The wide production and use of gold nanoparticles (AuNPs) in diverse applications (e.g. biomedical) may result in their continuous release to the environment (Khan, Vishakante, and Siddaramaiah 2013). Ultimately, aquatic ecosystems are the main recipients of AuNPs, mainly as a result of their release in industrial and domestic wastewaters (Piotrowska, Golimowski, and Urban 2009). AuNPs release may occur as early as during their production, the production of products containing nanoparticles, or during the use and end of life of those products. However, the currently available information in terms of the levels of

AuNPs in the environment is limited to predicted concentrations (aquatic compartment: 0.14 µg.L^{-1}), which have been estimated based on the use of NPs in consumer products (García-Negrete et al. 2013; Tiede et al. 2009).

Some studies have highlighted the possible toxic effects of AuNPs to aquatic organisms, that include oxidative stress, cytotoxicity, genotoxicity and protein modifications (Barreto et al. 2019a; Barreto et al. 2019b; Botha et al. 2015; Dedeh et al. 2015; García-Cambero et al. 2013; García-Negrete et al. 2013; Iswarya et al. 2016; Tedesco et al. 2010; Teles et al. 2016). Therefore, AuNPs may become a significant environmental concern as they can accumulate in organisms along aquatic food webs. Thus, there is the need of more research to improve our understanding of the toxicity of nanoparticles (NPs) in aquatic organisms, for instance using more holistic approaches. In this regard "OMICS" disciplines such as transcriptomics and proteomics provide unique opportunities to investigate and identify the mechanisms underlying nanotoxicity (Matysiak et al. 2016). Some studies have already shown that proteomics is a promising research discipline to evaluate toxicity of NPs, showing potential to reveal initiating and key molecular events related to NPs adverse outcomes (Gioria et al. 2014, 2016; Mirzajani et al. 2014a, 2014b; Otelea and Rascu 2015; Planchon et al. 2017).

A proteomic approach has already been employed to assess the effects of AuNPs in human adenocarcinoma Caco-2 cells (Gioria et al. 2016), Balb/3T3 mouse fibroblast cell line (Gioria et al. 2014) and the mussel *Mytilus edulis* (Tedesco et al. 2010). However, only two proteomic studies were conducted aiming to assess the toxicity of NPs in fish, using the liver (Gupta et al. 2016; Naderi et al. 2017). A 7 d exposure to copper NPs (100 µg.L^{-1}) induced differences in the abundance of proteins associated with oxidative stress and steroid biosynthesis in *Cyprinus carpio* (Gupta et al. 2016). Selenium NPs (1 mg.kg^{-1}; 60 d of exposure) altered the abundance of proteins associated with glycolysis, gluconeogenesis and amino acid metabolism in *Oncorhynchus mykiss* (Naderi et al. 2017). However, to our knowledge no proteomics studies have been performed to assess the effects of AuNPs in fish.

The present study aimed to understand the toxic effects of a 96 h exposure to 7 and 40 nm AuNPs, with citrate or polyvinylpyrrolidone (PVP) coating, on the gilthead

seabream (*S. aurata*) liver proteome, using a gel-based proteomics approach. *S. aurata*, a marine top predator fish, was selected as aquatic model organism in this study since it is a species with a wide geographic distribution and an important economic resource in the European aquaculture industry (Cordero et al. 2016). Thereby the results of this study will also contribute to predict the impacts of NPs in the aquaculture sector in Europe and worldwide. The physicochemical properties of NPs, especially size and surface coating, are considered important factors that influence directly and significantly the toxicity of NPs (Khanna et al. 2015). To date, a few studies with *S. aurata* (liver) have investigated the effects of different commercial foods (Ghisaura et al. 2014), maslinic acid (Rufino-Palomares et al. 2011) and ivermectin (Varo et al. 2010). However, to the best of our knowledge this is the first study addressing the effects of AuNPs on the proteome of this marine/estuarine fish species. The liver was investigated since this organ play a major role in several key metabolic processes involved in the detoxification of different types of substances and xenobiotics (Alves et al. 2010) and accumulation of AuNPs (Chen et al. 2013; Iswarya et al. 2016; Khan, Vishakante, and Siddaramaiah 2013; Mateo et al 2014; Simpson et al. 2013). Moreover, Barreto et al. (2019b) showed previously that, *S. aurata* exposed to the same AuNPs, the highest gold bioaccumulation factor was observed in the liver.

2. Material and Methods

2.1. Fish maintenance

Juvenile gilthead seabream (*S. aurata*), length 7.7 ± 0.6 cm, were purchased from a Spanish aquaculture facility and were acclimated in the laboratory for 4 weeks in aquaria containing aerated and filtered artificial seawater (ASW, salinity 30), under controlled temperature (18ºC) and natural photoperiod. During this period, fish were fed daily with commercial fish food (Sorgal, Portugal) and the aquaria water was renewed daily. All experimental procedures were carried out following the European and Portuguese legislation (authorization N421/2013 of Portuguese competent authority). Animal handling was performed by an accredited researcher. During the experimental assay, photoperiod, temperature and aeration conditions were similar to those used in the acclimation period.

2.2. Gold nanoparticles (AuNPs) synthesis and characterisation

Citrate-coated AuNPs (cAuNPs) with 7 nm diameter were synthesized by pH-shifting method, with reduction of gold (III) chloride trihydrate by citric acid, followed by neutralization with NaOH (Shiba 2013). cAuNPs with 40 nm diameter were prepared, using 15 nm seeds, by sodium citrate reduction of gold (III) chloride trihydrate (Lekeufack et al. 2010). Part of the cAuNPs were coated with PVP as described by Barreto et al. (2015). The citrate reduction method was chosen because: 1) it has been widely used; 2) the non-toxicity of citrate; 3) the use of water as solvent (Hanžić et al. 2015; Li et al. 2011; Turkevich, Stevenson, and Hillier 1951). PVP was selected as a second coating and stabilizing agent because it is a water-soluble, nontoxic and biodegradable homopolymer (Min et al. 2009). After synthesis, the AuNPs stock suspensions in ultrapure water and in ASW were characterised by UV-Vis spectra (Cintra 303, GBC Scientific), dynamic light scattering (DLS; Zetasizer Nano ZS, Malvern), transmission electron microscopy (TEM; Hitachi, H9000 NAR), scanning electron microscopy (SEM; Hitachi, SU70) and zeta potential (ZP; Zetasizer Nano ZS, Malvern).

2.3. Experimental assay and sampling biological material

The procedures were based on the OECD guideline (number 203) for fish acute bioassays (OECD 1992). Briefly, 9 fish per condition (6 for proteomic analysis and 3 for gold quantification) were randomly distributed across experimental aquaria (3 replicate tanks per condition) in the ratio 1 g of fish per 1 L of ASW and exposed for 96 h, as recommended by the guideline, to the following 5 conditions: control (only ASW); 80 $\mu g.L^{-1}$ of 7 nm cAuNPs; 80 $\mu g.L^{-1}$ of 7 nm PVP-AuNPs; 80 $\mu g.L^{-1}$ of 40 nm cAuNPs and 80 $\mu g.L^{-1}$ of 40 nm PVP-AuNPs. Experimental suspensions of AuNPs were prepared by dilution of AuNPs stock suspensions in ASW. The AuNPs concentration, 80 $\mu g.L^{-1}$, was chosen since this concentration was previously shown to exert potential toxic effects in *S. aurata*. In earlier studies, AuNPs at 80 $\mu g.L^{-1}$ were able to induce DNA damage (erythrocyte DNA strand breaks) and increase erythrocytic nuclear abnormalities levels (Barreto et al. 2019a), as well as to affect the hepatic expression of antioxidant, immune and apoptosis related genes in *S. aurata* (Teles et al. 2016).

Approximately 80% of the experimental media was renewed daily after checking fish mortality and behaviour and measuring water quality (temperature, salinity, conductivity, pH and dissolved oxygen). No food was provided during the experimental period, as recommended by the guideline number 203. Water samples were collected daily (at 0 and 24 h), from each experimental aquarium, for the gold quantification. Water samples collected at 0 h, correspond to the water collected at the beginning of the assay (day 0) and at each day after the renewal of the media (day 1 to 3). Water samples collected at 24 h, correspond to the water collected at each day before the renewal of the media (day 1 to 3) and at 96 h after the beginning of the test (day 4).

After 96 h exposure, animals were anesthetized with tricaine methanesulfonate (MS-222) and euthanized by spinal section. Liver was removed from 6 fish and stored at -80ºC until proteome analysis. Liver, gills, spleen and muscle were taken from 3 animals and kept at -20ºC until gold quantification. These four tissues were selected based on the reported accumulation of silver in *Cyprinus carpio* waterborne exposed to silver NPs (Lee et al. 2012). At the time the tissues were chosen, a single study had focused on the accumulation of gold metal in fish after waterborne exposure to AuNPs; however, this study only assessed body content in the marine fish *Pomatoschistus microps* (Ferreira et al. 2016).

2.4. Gold quantification

The determination of gold in the stock suspensions, the experimental media and fish tissues was performed according to NIST NCL Method PCC-8 (NIST 2010). All the samples were acid digested and a MLS-1200 Mega microwave digestion unit (Milestone, Sorisole, Italy) was used for closed-vessel acid digestion of the fish samples. An iCAP™ Q ICP-MS (inductively coupled plasma mass spectrometry; Thermo Fisher Scientific; Bremen, Germany) was used for gold determination in both fish digests and water samples. The ICP-MS instrumental conditions were as follow: argon flow rate (14 $L.min^{-1}$); auxiliary argon flow rate (0.8 $L.min^{-1}$); nebulizer flow rate (1.03 $mL.min^{-1}$); RF power (1550 W) and dwell time (100 ms). The elemental isotope ^{197}Au was monitored for analytical determination; ^{159}Tb and ^{209}Bi

were used as internal standards. The instrument was tuned daily for maximum signal sensitivity and stability.

2.5. Total gold content and bioaccumulation factor

Total gold content ($[Au]_{total}$), in µg.g^{-1}, was calculated as the sum of the gold content in each assessed tissue of the fish according to the formula:

$$[Au]_{total} = [Au]_g + [Au]_l + [Au]_s + [Au]_{ms}$$

Where $[Au]_g$ is the concentration of gold in gills, $[Au]_l$ the concentration of gold in liver, $[Au]_s$ the concentration of gold in spleen and $[Au]_{ms}$ the concentration of gold in muscle.

The bioaccumulation factor (BAF), in L.g^{-1}, was calculated according to Yoo-Iam et al (2014), dividing the gold content (µg.g^{-1}) in each tissue of the fish (gills, liver, spleen or muscle) by the initial concentration of gold in the exposure media (µg.L^{-1}):

$$BAF = [Au]_t / [Au]_{ASW}$$

Where $[Au]_t$ is the content of gold in the specific fish tissue and $[Au]_{ASW}$ is the concentration in the exposure media – ASW (collected daily at 0 h and quantified).

2.6. Liver proteome analysis

2.6.1. Protein extraction

Proteins were extracted from liver samples following a protocol adapted from Campos et al. (2013). Briefly, each liver tissue (~ 0.1 g) was mixed in 1 mL of extraction buffer with 7 M urea, 2 M thiourea, 4% (w/v) CHAPS, 65 Mm DTT (1,4-dithiothreitol), 0.8% (v/v) ampholytes IPG (immobilized pH gradient) Buffer pH 3-10 and 1% (v/v) protease inhibitor, homogenized with a probe sonicator (Vibra-CellTM, Sonics & Materials) and the homogenate incubated for 1 h, under agitation, at room temperature. After centrifugation (17 000 x g, for 10 min, at room temperature) proteins were precipitated with a solution containing 10% (w/v) trichloroacetic acid (TCA), acetone and 0.07% (v/v) β-mercaptoethanol (β-ME) in a 1:10 (v/v) ratio of

sample and precipitation solution. This mixture was left at -20˚C for 1 h and then centrifuged (16 000 x g for 20 min at 4˚C). After discarding the supernatant, the protein pellet was washed twice with 0.07% β-ME in acetone. Afterwards, the protein pellet was allowed to dry at room temperature for 1 h, resuspended in extraction buffer with agitation for 20 min and centrifuged (15 000 x g for 20 min at room temperature). The supernatant was then recovered and stored at -20˚C. Protein concentration was determined according to the Bradford method, adapted to microplate, using bovine serum albumin (BSA) as standard.

2.6.2. Two-dimensional gel electrophoresis (2-DE)

Protein extracts (400 µg) were diluted in 300 µL extraction buffer and applied to 17 cm (pH 3-10) ReadyStrip IPG Gel Strips (Bio-Rad). The first dimension (isoelectric focusing) was carried out in a Protean IEF Cell (Bio-Rad). The gel strips were actively rehydrated for 14 h (50 V). After rehydration, voltage was set at constant 250 V for 15 min, followed by a linear increase to 10 000 V for 3 h and then a linear increase up to 60 000 V for the complete separation of proteins. A 500 V was applied to the system until the gel strips were stored at -20ºC.

IPG gel strips were incubated, for 15 min, in equilibration solution 1 (50 mM Tris-HCl, 6 M urea, 30% (v/v) glycerol, 2% (w/v) sodium dodecyl sulfate (SDS) and 1% (w/v) DTT under slow agitation. The solution was drained and gel strips incubated again with equilibration solution 2 (50 mM Tris-HCl, 6 M urea, 30% (v/v) glycerol, 2% (w/v) SDS and 2.5% (w/v) iodoacetamide) for 15 min. Once this step was completed, the gel strips were washed in electrophoresis buffer (24.8 mM Tris-HCl, 192 mM glycine and 0.1% (w/v) SDS) and assembled in SDS-PAGE gels. The second dimension (SDS-PAGE – sodium dodecyl sulfate polyacrylamide gel electrophoresis) was performed in 12% (w/v) acrylamide gels, using a Hoefer SE900 multi-gel system (Hoefer, Inc.). The electrophoresis ran overnight, with constant voltage (80 V) at 16˚C. When second dimension finished, gels were stained with Coomassie Blue Colloidal stain, according to Neuhoff et al. (1988).

2.6.3. Quantitative analysis of gel images and statistics

Gels were scanned using a GS-800 Calibrated Densitometer (Bio-Rad). To analyse differences in the protein patterns between the five conditions (control and the treatments with AuNPs), the PDQuest 8.0 software (Bio-Rad) was used. An initial automatic detection and matching of the protein spots, applying the same sensitivity parameters for all gels, followed by manual inspection of matched spots were performed. Mismatched protein spots were then corrected, and spot artefacts eliminated from the analysis. Four 2-DE gels per experimental condition were analysed. Protein spot densities were normalized by the software, according to their total density. The spot densities were subsequently used as a measure of protein abundance in the sample.

Only spots exhibiting abundance ratios of at least 3.0-fold change with respect to the control were considered. To increase the confidence of this analysis, spots without quantitative information in at least three gel replicates in each condition were ignored. Additionally, one-way analysis of variance (ANOVA) followed by Dunnett's test, whenever applicable, was performed using JMP 12 software (SAS Institute, USA). Significant differences were assumed for $p<0.05$. The heat map, based on the abundance of each protein, was obtained using the program Multiple Experient Viewer (https://www.mybiosoftware.com/mev-4-6-2-multiple-experiment-viewer.html).

2.6.4. Protein identification and functional analysis

Protein spots were excised from 2-DE gels and proteins subjected to in-gel digestion using the protease trypsin (Pandey and Mann 2000). The tryptic digests were desalted, concentrated using reversed phase micro-columns (Gobom et al. 1999) and directly eluted onto the matrix-assisted laser desorption/ionization (MALDI) plate with the matrix α-cyano-4-hydroxycinamic acid (5 $mg.mL^{-1}$) in 70% acetonitrile (v/v) and 0.1% trifluoroacetic acid (v/v). Peptides were analysed by MALDI-TOF/TOF (matrix assisted laser desorption/ionisation time of flight; 4800 MALDI-TOF/TOF Analyser, SCIEX, Framingham, MA) in MS and MS/MS mode and employing collision induced dissociation – CID fragmentation method. The collision energy was set to 1 keV. Up to ten S/N (signal-to-noise ratio) precursors from each MS spectrum were selected for MS/MS analysis. The generated mass spectra were

searched against all sequences from species of the class *Actinopterygii* available in the Uniprot database (1434448 sequences, January 2018) or the *Danio rerio* sequences, using the algorithm MOWSE, from MASCOT server 2.3 (Matrix Science, UK) using the Peptide Mass Fingerprint (PMF) approach combined, whenever possible, with MS/MS peptide sequencing. Up to two trypsin missed cleavages, carbamidomethylation of cysteine as fixed modification as well as four dynamic modifications (methionine and tryptophan oxidation, tryptophan deoxidation and tryptophan tokynurenin) were allowed. Mass accuracy was set to 50 ppm for parent ions and 0.5 Da for MS/MS fragments. Significance threshold was set to $p<0.05$. The molecular functions and biological processes of the differential proteins were retrieved from the UNIPROT database (https://www.uniprot.org/), after searching the full description of each protein using the respective accession numbers or, alternatively, searching the full description of homologous protein in Humans. Moreover, a functional analysis of the differential proteins was carried out using the web resource STRING (https://string-db.org/). The analysis was carried out using Human homologues as references genes. Human gene identifiers were retrieved from UNIPROT database (https://www.uniprot.org/) and after searching for Human proteins with names identical to the proteins identified by proteomics. In case of doubt, a BLAST search was carried out (E-threshold < 10e-10) to help to find the corresponding homologous protein in Humans and the respective gene identifier. STRING analysis was performed with the following settings: organism – *Homo sapiens*; sources of evidence – text mining, experiments, databases, co-expression, neighborhood, gene fusion, co-occurrence; interaction score – medium confidence (0.400); max number of interactors (1st shell): no more than 5.

3. Results and Discussion

3.1. Gold nanoparticles (AuNPs) – Characterisation

Microscopy analysis confirmed that AuNPs presented a spherical shape (Figure 1), had the expected sizes (around 7 and 40 nm) and allowed the visualization of a PVP layer around the metal core of AuNPs (Figure 1B and D).

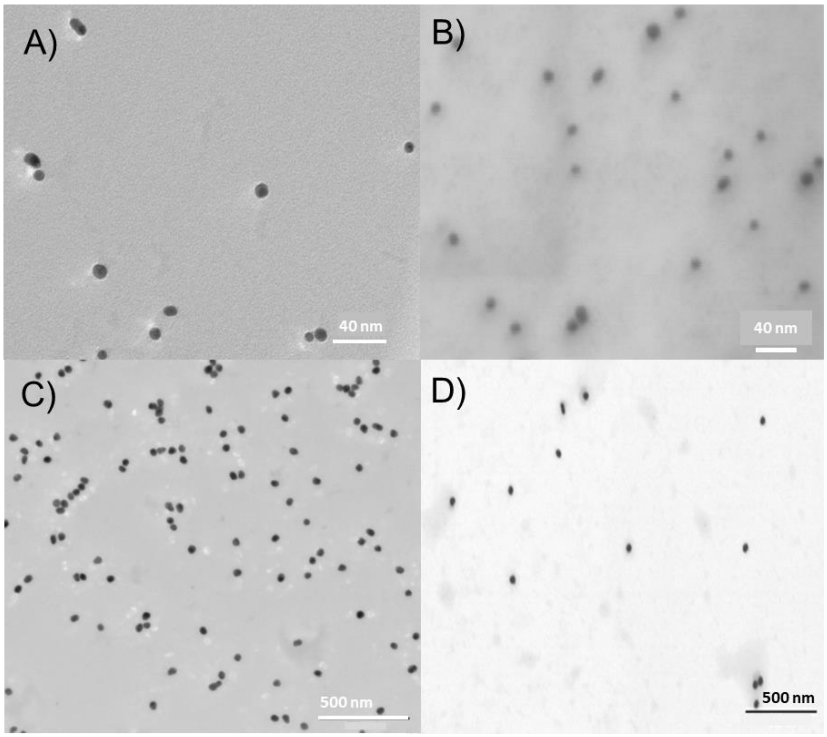

Figure 1 – Electron microscopy images of 7 and 40 nm citrate (cAuNPs) and polyvinylpyrrolidone (PVP-AuNPs) gold nanoparticles stock suspensions in ultrapure water: **A)** 7 nm cAuNPs (98 mg.L^{-1}); **B)** 7 nm PVP-AuNPs (51 mg.L^{-1}); **C)** 40 nm cAuNPs (97 mg.L^{-1}); **D)** 40 nm PVP-AuNPs (58 mg.L^{-1}).

In ASW, at 800 µg.L^{-1}, ten times greater than the tested concentration, cAuNPs (7 and 40 nm) changed their typical colour red/pink to light blue. The hydrodynamic size of 7 and 40 nm cAuNPs increased to around 160 and 430 nm, respectively, maintaining the respective sizes for 96 h (the duration of the test). The characteristic SPR peak of the cAuNPs detected in ultrapure water (Table 1) was not detected in ASW, which was likely due to agglomeration/aggregation of AuNPs. Additionally, different peaks corresponding to different charges were found in the ZP analysis. Concerning 7 and 40 nm PVP-AuNPs, no colour alteration was observed in ASW. PVP-AuNPs in ASW had similar characteristics as the PVP-AuNPs in ultrapure water (Table 1). A previous study (Barreto et al. 2015) demonstrated that PVP-AuNPs were stable in ASW for more than 30 d whereas cAuNPs immediately altered their characteristics and aggregated/agglomerated, increasing their size. These characteristics (size and surface coating) may thus influence NPs bioavailability, accumulation and toxicity. At 80 µg.L^{-1} it was not possible to characterise the AuNPs

since the detection limits of the techniques used to characterise the NPs are above the exposure concentration. However, it was possible to see that 7 nm cAuNPs, when in ASW, immediately changed their typical colour, from red to light blue, as a result of AuNPs agglomeration/aggregation, whereas 7 nm PVP-AuNPs did not show colour alteration. Concerning 40 nm AuNPs, no change of colour in ASW was observed. This may be explained by the fact that, for the same concentration, 7 nm AuNPs suspension presented a higher number of particles than the 40 nm AuNPs suspension. Agglomeration/aggregation of NPs was expected to increase with the increase in the number of particles per volume (Barreto et al. 2015). The surface energy of AuNPs increases as the NPs diameter decreases. Thus, smaller AuNPs may interact more strongly with other compounds present in the medium leading to size-dependent aggregation/agglomeration of AuNPs (Iswarya et al. 2016; Zeng et al. 2012).

Table 1. Characteristics of gold nanoparticles (AuNPs) stock suspensions in ultrapure water. cAuNPs – Citrate coated gold nanoparticles; PVP-AuNPs – Polyvinylpyrrolidone coated gold nanoparticles; PdI – Polydispersity Index; SPR – Surface plasmon resonance; ZP – Zeta potential.

	Concentration ($mg.L^{-1}$)	**Size (nm)**	**PdI**	**SPR (nm)**	**ZP (mV)**	**pH**
7 nm cAuNPs	98	6.7	0.5	519	-43.3	6.4
7 nm PVP-AuNPs	51	7.6	0.5	521	-12.8	6.9
40 nm cAuNPs	97	35.0	0.3	534	-44.1	5.9
40 nm PVP-AuNPs	58	50.3	0.3	535	-17.2	6.4

3.2. Gold quantification in the test media

The amount of gold quantified in the experimental medium (ASW) was generally lower than the nominal concentration (80 $\mu g.L^{-1}$). At 0 h, the measured concentrations of gold were around 20 $\mu g.L^{-1}$, with the exception of the experimental medium containing 40 nm cAuNPs, where 10 $\mu g.L^{-1}$ of gold was quantified (Table 2). After 24 h of exposure, comparing with the levels of gold quantified at 0 h, gold

concentration decreased more in the experimental medium containing cAuNPs than in that containing PVP-AuNPs (Table 2). For 7 nm cAuNPs and PVP-AuNPs exposures, a 59 and 18% decrease in gold content was found, respectively. For 40 nm cAuNPs and PVP-AuNPs exposures, the concentrations of gold decreased by 37 and 27%, respectively. The higher decrease of gold, observed after 24 h in the experimental medium containing cAuNPs, may be explained by the effect of aggregation/agglomeration of these particles in ASW and subsequent sedimentation. As PVP-AuNPs may remain stable in ASW for 24 h, the concentration of gold in the experimental medium containing these particles, was closer to the initial concentration comparing with experimental medium with cAuNPs.

Table 2. Gold concentrations ($\mu g.L^{-1}$) measured on the experimental media containing 7 and 40 nm gold nanoparticles (citrate coated – cAuNPs and polyvinylpyrrolidone coated – PVP-AuNPs) at 0 and 24 h. Results are expressed as mean ± standard error.

Size AuNPs (nm)	Time (h)	Gold concentration ($\mu g.L^{-1}$) cAuNPs	PVP-AuNPs
7	**0**	20.6 ± 0.1	22.7 ± 0.2
	24	8.4 ± 0.1	18.7 ± 0.1
40	**0**	10.1 ± 0.1	22.5 ± 0.1
	24	6.4 ± 0.1	16.5 ± 0.2

3.3. Total gold content and bioaccumulation factor

Gold significantly accumulated in all investigated tissues (gills, liver, spleen and muscle) after exposure to 7 nm PVP-AuNPs ($p<0.05$; Dunnett's test; Table 3). The exposure to 7 nm cAuNPs and 40 nm PVP-AuNPs also resulted in significant gold accumulation in all investigated tissues ($p<0.05$; Dunnett's test; Table 3), except in muscle. However, in the 40 nm cAuNPs exposure, gold only accumulated significantly in the liver ($p<0.05$; Dunnett's test; Table 3).

Table 3. Gold concentration in tissues of *Sparus aurata* (gills, liver, spleen and muscle) exposed to 7 and 40 nm gold nanoparticles (citrate coated – cAuNPs and

polyvinylpyrrolidone coated – PVP-AuNPs) for 96 h and respective estimated bioaccumulation factor (BAF). Results are expressed as mean ± standard error. *Significant differences to control (Dunnett´s test, $p<0.05$). $[Au]_{total}$ – Total gold content. b.d.l. – Bellow the detection limit.

Size AuNPs (nm)	Tissues	Gold Content ($\mu g.g^{-1}$)		BAF ($L.g^{-1}$)	
		cAuNPs	PVP-AuNPs	cAuNPs	PVP-AuNPs
7	**Gills**	1.9 ± 0.1 *	6.3 ± 0.1 *	0.1	0.3
	Liver	7.8 ± 0.1 *	9.8 ± 0.1 *	0.4	0.4
	Spleen	17.4 ± 0.2 *	15.8 ± 0.1 *	0.8	0.7
	Muscle	b.d.l.	2.2 ± 0.1 *	-	0.1
	[Au]total	**27.1 ± 0.1**	**34.1 ± 0.1**	**1.3**	**1.5**
40	**Gills**	0.11 ± 0.0	3.6 ± 0.1 *	0.0	0.2
	Liver	0.7 ± 0.0 *	1.4 ± 0.1 *	0.1	0.1
	Spleen	b.d.l.	17.7 ± 0.1 *	-	0.8
	Muscle	b.d.l.	b.d.l.	-	-
	[Au]total	**0.8 ± 0.1**	**22.7 ± 0.0**	**0.1**	**1.1**
Control	**Gills**	b.d.l.	b.d.l.	-	-
	Liver	b.d.l.	b.d.l.	-	-
	Spleen	b.d.l.	b.d.l.	-	-
	Muscle	b.d.l.	b.d.l.	-	-
	[Au]total	-	-	-	-

The total gold accumulation in fish after the exposure to 7 and 40 nm PVP-AuNPs was approximately 34 $\mu g.g^{-1}$ and 23 $\mu g.g^{-1}$, respectively (Table 3). Gold accumulated more (approximately 30%) in fish exposed to 7 nm PVP-AuNPs than in those exposed to 40 nm PVP-AuNPs. However, this difference was more significant in the exposure to cAuNPs: approximately 27 $\mu g.g^{-1}$ and 1 $\mu g.g^{-1}$ to 7 and 40 nm, respectively (Table 3).

In the case of 7 nm AuNPs, gold accumulation in fish was similar regardless its coating compound (citrate: approximately 27 $\mu g.g^{-1}$ and PVP: approximately 34 $\mu g.g^{-1}$; Table 3). Nevertheless, concerning 40 nm AuNPs, gold accumulation was dependent on the coating, with higher gold accumulation observed after exposure to PVP-AuNPs (23 $\mu g.g^{-1}$) than after cAuNPs exposure (1 $\mu g.g^{-1}$; Table 3).

Overall, taking into account all exposures, the accumulation of gold in the different tissues analysed may be ranked as follow: spleen>liver>gills>muscle. In fish, spleen plays an important hematopoietic function. It is one of the major immune organs that can trap and clear foreign particulate material and maintain stable internal

environment (Rønneseth, Wergeland, & Pettersen, 2007). The accumulation of gold in this tissue can be adverse to many important physiological processes (Kondera et al., 2014), which subsequently can disturb homeostatic mechanisms, such as the antioxidant system and fish immune system (Coles et al., 1995). Chen et al. (2009) showed that the accumulation of gold in the spleen of mammals, after the exposure to AuNPs, led to splenic toxicity (Chen et al. 2009). The $[Au]_{total}$ values and the calculated BAF may be ranked as follow: 7 nm PVP-AuNPs>7 nm cAuNPs>40 nm PVP-AuNPs>40 nm cAuNPs (Table 3). Taking into account the sizes of the AuNPs tested, the accumulation of gold was higher after the exposure to the smallest tested AuNPs – 7 nm. It has already been described that the size of NPs may influence their accumulation in organisms with smaller AuNPs showing higher levels of accumulation (Bajak et al. 2015; Huang et al. 2012).

The higher accumulation of gold in tissues when fish were exposed to PVP-AuNPs is probably related to increased bioavailability of PVP-AuNPs, relatively to cAuNPs. The characterisation of PVP-AuNPs (800 $\mu g.L^{-1}$), at 0 and 96 h, showed that these NPs were the most stable in ASW, maintaining their nano size, being dispersible in the water column, which may favour the uptake by fish. On the contrary, cAuNPs (800 $\mu g.L^{-1}$) aggregate/agglomerate and deposit on the tank bottom, leading to a lower concentration of AuNPs in the water column and, consequently, a lower uptake by fish. As previously reported, when NPs aggregate/agglomerate they become too large to be transported across the cell membrane, and uptake may be reduced (Vale et al. 2016). Also important for the interpretation of results, is that NPs properties may change inside the organism given the changes of the physico-chemical characteristics of the environment (e.g., presence of electrolytes and proteins, different pH) which could lead to the dissolution of some types of NPs. This, however, seems unlikely to occur in the case of AuNPs, since even at the lowest pH inside the fish (e.g. gastric pH), cAuNPs and PVP-AuNPs have been shown to aggregate/agglomerate, on the contrary dissolution has not been reported (Dhumale et al. 2012). Therefore, the possible effects caused by the AuNPs will be due to the nano form and not to the ionic form.

3.4. Two-dimensional gel electrophoresis (2-DE) gels

Thirty 2-DE gels (six gels per condition, corresponding to six individual livers) were performed to analyse the effects of AuNPs on the liver proteome of *S. aurata* after 96 h exposure. From the six gels per condition obtained, the four gels with highest quality were chosen to analyse protein expression. Gel selection was based on the quality of the protein profiles revealed in the gels and the number of proteins separated and visualised. In total, 632 protein spots were detected from 2-DE gels. This number of protein spots is within the range of protein spots commonly resolved by the technique. Large size 2-DE gels have been previously shown to resolve, with good accuracy, between 600 and 1000 protein spots (Osório et al. 2017).

Moreover, all gels showed similar staining intensities meaning that gels were correctly normalized in terms of protein amount (equal amount of protein loaded in each gel). A representative 2-DE gel is displayed in Figure 2. As can be seen on this gel, the majority of protein spots detected were distributed along the isoelectric point (pI) 7 and 10 and the molecular masses 20 and 70 kDa. The protein profiles revealed in these gels are consistent with a previous 2-DE proteomic profile from the liver of *S. aurata* in which 564 proteins were resolved along a pI gradient of 3 to 10 and molecular masses of 19 to 115 kDa (Rufino-Palomares et al. 2011).

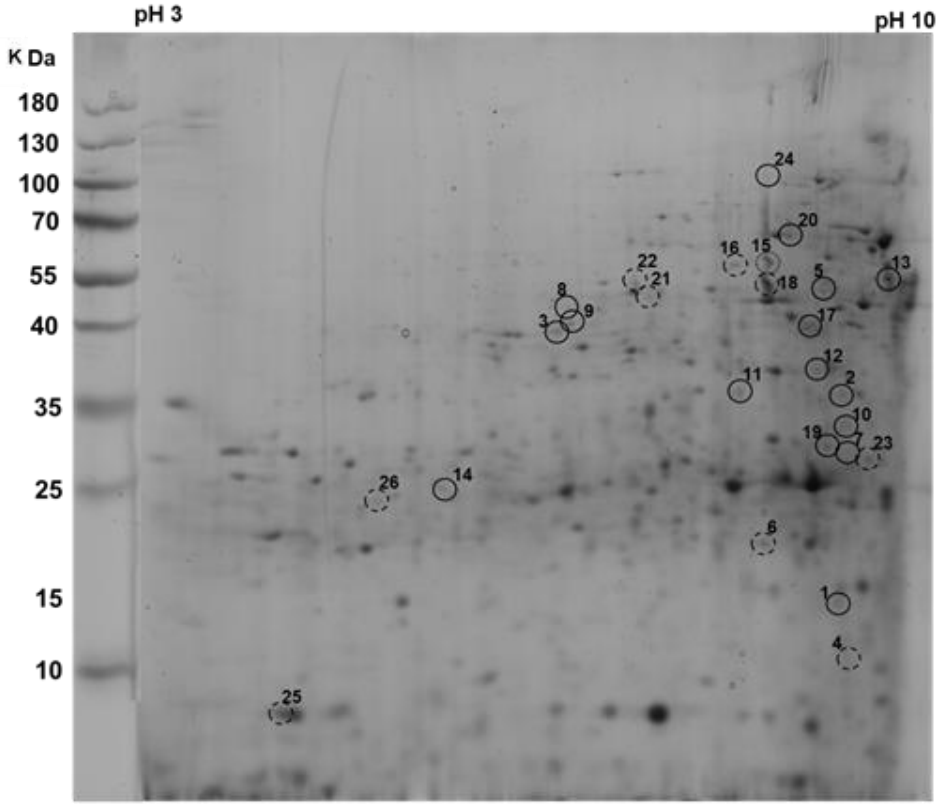

Figure 2. Proteomic map of *Sparus aurata* liver. Protein identities corresponding to the numbers indicated in the figure are reported in Table 4. Proteins were separated in the first dimension with pH 3–10 (IPG) immobilized pH gradient strips, followed by SDS-PAGE (sodium dodecyl sulfate polyacrylamide gel electrophoresis) on 12% w/v gels. Gels were stained with Coomassie Blue Colloidal. The 26 spots excised for MALDI-TOF/TOF MS (matrix assisted laser desorption/ionisation time of flight mass spectrometry) analysis are encircled. ◌ – down-regulated; ◯ – up-regulated; ◌ – down- or up-regulated

3.5. Proteins displaying differences in abundance

Of the 632 spots detected, 26 exhibited differences in abundance (either 3.0-fold changes or statistical differences at $p<0.05$, compared with the control) after the exposure to AuNPs. The 26 proteins displaying differences in abundance were marked on the reference 2-DE gel (Figure 2).

7 nm cAuNPs altered the abundances of 13 proteins (9 up- and 4 down-regulated), while 7 nm PVP-AuNPs (5 up- and 5 down-regulated) and 40 nm cAuNPs (6 up- and 4 down-regulated) altered abundances of 10 proteins and PVP-

AuNPs of 7 proteins (1 up- and 6 down-regulated) (Figure 3). Of the 26 proteins displaying differences in abundance, 17 were affected only by one of the treatments (eight by 7 nm cAuNPs; four by 7 nm PVP-AuNPs; three by 40 nm cAuNPs and two by 40 nm PVP-AuNPs) and nine proteins were affected by, at least, two of the treatments, with two proteins being affected by all AuNPs treatments (Figure 3). The 7 nm cAuNPs induced most alterations in the proteome of *S. aurata* (Figure 3).

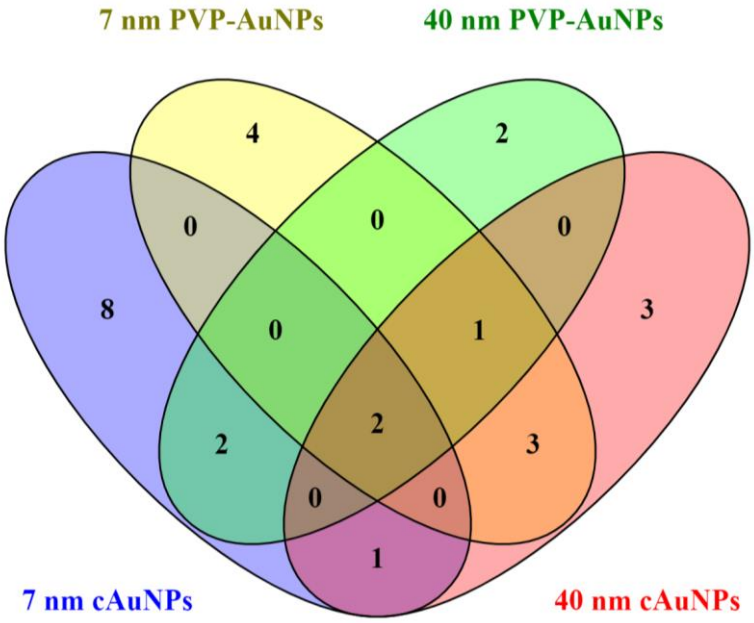

Figure 3. Venn diagram of the number of proteins displaying differences in abundance in *Sparus aurata* liver after 96 h exposure to gold nanoparticles (citrate coated – cAuNPs and polyvinylpyrrolidone coated – PVP-AuNPs), assessed by 2-DE.

Within this group of 26 proteins, 16 were up-regulated and 9 were down-regulated under the tested conditions (Table 4). One protein (number 15, actin) increased in abundance after exposure to 7 nm PVP-AuNPs but decreased after exposure to 40 nm cAuNPs. The protein numbers 16 and 21 (also actins) decreased in abundance regardless of the type of AuNPs fish were exposed (Table 4). To the best of our knowledge there are no studies concerning the effects of AuNPs in the fish liver proteome. However, previous studies already evaluated the effects of other types of NPs in the fish liver proteome (Gupta et al. 2016; Naderi et al. 2017). These studies reported alterations in the abundance of 30 and 15 proteins of the liver of

Cyprinus carpio and *Oncorhynchus mykiss* after the exposure to copper and selenium NPs, respectively (Gupta et al. 2016; Naderi et al. 2017).

Table 4. Proteins displaying differences in abundance in *Sparus aurata* liver after 96 h exposure to gold nanoparticles (citrate coated – cAuNPs and polyvinylpyrrolidone coated – PVP-AuNPs), assessed by 2-DE. Values of protein expression are represented as mean spot density estimated from four replicate gels ± standard error. *Significant differences to control (Dunnett´s test, $p<0.05$). #3.0-fold changes to control. Proteins identified with *Danio rerio* and *Actinopterygii* databases. (1) Uniprot database accession numbers. ID – Identification; MS – Mass Spectrometry; MS/MS – Tandem-Mass Spectrometry; – Up-regulated; – Down-regulated.

		Protein Expression									Matched Peptides	
Protein Number	**Gene ID**	**Control**	**7 nm cAuNPs**	**7 nm PVP-AuNPs**	**40 nm cAuNPs**	**40 nm PVP-AuNPs**	**Protein Name**	**Accession Number (1)**	**Species**	**Protein Score**	**MS**	**MS/ MS**
1	EEF1G	1129.3 ± 287.4	2935.7 ± 1462.8*	726.2 ± 350.8	1250.3 ± 299.3	459.6 ± 279.2	Elongation factor 1-gamma	A0A0F8C4B3	*Larimichthys crocea*	80	58	0
2	HSP90	694.8 ± 201.3	1129.1 ± 835.6*	518.8 ± 303.7	254.4 ± 207.7	295.0 ± 119.4	94 kDa glucose-regulated protein	M9NZ74	*Sparus aurata*	200	34	4
3	PCK2	805.0 ± 206.8	1858.1 ± 559.2*	1110.1 ± 654.5	1851.8 ± 882.2*	707.7 ± 181.1	Phosphoenolpyruvate carboxykinase 2 (mitochondrial)	F1R9Y5	*Danio rerio*	73	22	1
4	GKUP	695.2 ± 349.5	525.2 ± 177.3	10.2 ± 10.2*	955.1 ± 417.9	594.0 ± 442.2	Glucuronokinase with putative uridyl pyrophosphorylase	A0A0R4IGN7	*Danio rerio*	86	34	0
5	ATP5B	451.4 ± 168.5	247.6 ± 148.4	1291.2 ± 798.7	2056.9 ± 1088.7*	302.2 ± 175.5	ATP synthase subunit beta	A8WGC6	*Danio rerio*	396	30	6
6	SHMT2	926.5 ± 321.9	277.1 ± 277.1	1640.8 ± 1057.9	1245.3 ± 426.4	76.9 ± 76.9*	Mitochondrial serine hydroxymethyltransferase	A9LDD9	*Danio rerio*	95	17	3
7	CPA	0.0 ± 0.0	226.4 ± 226.4	923.7 ± 319.5*#	135.5 ± 135.5	0.0 ± 0.0	Carboxypeptidase	G3NFY9	*Gasterosteus aculeatus*	144	7	2
8	PC	0.0 ± 0.0	0.0 ± 0.0	50.6 ± 50.6	117.3 ± 117.3*#	100.4 ± 100.4	Pyruvate carboxylase b	B0S5R6	*Danio rerio*	71	19	1
9	SELENBP1	277.7 ± 109.4	88.1 ± 88.1	644.7 ± 406.0*	621.2 ± 441.2*	549.7 ± 120.6	Selenium-binding protein 1	Q6PHD9	*Danio rerio*	138	11	3

Table 4 (continuation). Proteins displaying differences in abundance in *Sparus aurata* liver after 96 h exposure to gold nanoparticles (citrate coated – cAuNPs and polyvinylpyrrolidone coated – PVP-AuNPs), assessed by 2-DE. Values of protein expression are represented as mean spot density estimated from four replicate gels ± standard error. *Significant differences to control (Dunnett´s test, p<0.05). #3.0-fold changes to control. Proteins identified with *Danio rerio* and *Actinopterygii* databases. (1) Uniprot database accession numbers. ID – Identification; MS – Mass Spectrometry; MS/MS – Tandem-Mass Spectrometry; – Up-regulated; – Down-regulated.

		Protein Expression									Matched Peptides	
Protein Number	**Gene ID**	**Control**	**7 nm cAuNPs**	**7 nm PVP-AuNPs**	**40 nm cAuNPs**	**40 nm PVP-AuNPs**	**Protein Name**	**Accession Number (1)**	**Species**	**Protein Score**	**MS**	**MS/ MS**
10	TUBB2B	297.6 ± 297.6	1259.6 ± 444.7*	383.5 ± 224.9	0.0 ± 0.0	221.6 ± 173.9	Tubulin beta chain	Q32PU7	*Danio rerio*	124	21	4
11	TUBB2B	0.0 ± 0.0	0.0 ± 0.0	126.8 ± 126.8	0.0 ± 0.0	664.0 ± 322.1*#	Tubulin beta chain	Q32PU7	*Danio rerio*	169	20	2
12	CYTH1	340.5 ± 115.2	719.7 ± 486.8*	661.2 ± 309.1	485.3 ± 284.8	433.8 ± 201.7	Cytohesin-1	A0A146RY54	*Fundulus heteroclitus*	64	28	0
13	CALR	3174.4 ± 1340.4	1099.5 ± 476.3	142.3 ± 142.3*	1696.5 ± 660.1	733.5 ± 468.1	Calreticulin	F1Q8W8	*Danio rerio*	110	12	1
14	BHMT	101.0 ± 101.0	1100.4 ± 382.7*	223.8 ± 223.8	666.1 ± 262.3	250.9 ± 150.2	Betaine--homocysteine S-methyltransferase 1	F1QU55	*Danio rerio*	156	16	2
15	ACTBA	426.1 ± 371.4	902.7 ± 662.3	3935.9 ± 2108.4*	1933.9 ± 1378.2*	774.8 ± 366.2	Actin, cytoplasmic 1	Q7ZVI7	*Danio rerio*	528	22	7
16	ACTBA	2794.4 ± 2523.6	285.5 ± 285.5*	0.0 ± 0.0*	0.0 ± 0.0*	58.1 ± 58.1*	Actin, cytoplasmic 1	Q7ZVI7	*Danio rerio*	222	19	4
17	ACTBA	938.7 ± 592.3	979.8 ± 575.1	3794.2 ± 1889.1*	4371.8 ± 2139.1*	1559.7 ± 1258.0	Actin, cytoplasmic 1	Q7ZVI7	*Danio rerio*	309	15	5

Table 4 (continuation). Proteins displaying differences in abundance in *Sparus aurata* liver after 96 h exposure to gold nanoparticles (citrate coated – cAuNPs and polyvinylpyrrolidone coated – PVP-AuNPs), assessed by 2-DE. Values of protein expression are represented as mean spot density estimated from four replicate gels ± standard error. *Significant differences to control (Dunnett´s test, p<0.05) #3.0-fold changes to control. Proteins identified with *Danio rerio* and *Actinopterygii* databases. (1) Uniprot database accession numbers. ID – Identification; MS – Mass Spectrometry; MS/MS – Tandem-Mass Spectrometry; – Up-regulated; – Down-regulated.

		Protein Expression									Matched Peptides	
Protein Number	**Gene ID**	**Control**	**7 nm cAuNPs**	**7 nm PVP-AuNPs**	**40 nm cAuNPs**	**40 nm PVP-AuNPs**	**Protein Name**	**Accession Number (1)**	**Species**	**Protein Score**	**MS**	**MS/ MS**
18	ACTBA	2490.9 ± 1259.5	5749.4 ± 2359.8	6084.7 ± 2182.6*	4040.1 ± 1586.1	2275.9 ± 385.7	Actin, cytoplasmic 1	Q7ZVI7	*Danio rerio*	282	24	4
19	ACTBB	622.8 ± 68.7	486.6 ± 301.4	195.8 ± 195.8	682.6 ± 682.6*	130.0 ± 130.0	Actin, cytoplasmic 2	Q7ZVF9	*Danio rerio*	74	16	1
20	ACTBB	589.1 ± 239.2	1228.5 ± 1020.7*	292.7 ± 292.7	298.3 ± 298.3	102.1 ± 102.1	Actin, cytoplasmic 2	Q7ZVF9	*Danio rerio*	84	22	1
21	ACTBB	552.8 ± 494.1	235.4 ± 146.7*	0.0 ± 0*	0.0 ± 0.0*	78.2 ± 78.2*	Actin, cytoplasmic 2	Q7ZVF9	*Danio rerio*	84	18	2
22	FAH	922.8 ± 536.0	409.7 ± 541.5*	333.9 ± 270.8	109.5 ± 109.5	174.9 ± 112.8*	Fumarylacetoacetate hydrolase (Fumarylacetoacetase)	Q803S0	*Danio rerio*	165	14	3
23	HPCA	995.5 ± 995.5	722.4 ± 487.6	641.4 ± 641.4	905.5 ± 644.0	986.8 ± 437.0*	Hippocalcin	I3JLG1	*Oreochromis niloticus*	64	16	1
24	FGF1B	100.1 ± 58.5	943.4 ± 361.4*	158.0 ± 158.0	231.1 ± 231.1	61.8 ± 61.8	Fibroblast growth factor	A7YT71	*Danio rerio*	64	16	0
25	PPIA	2107.6 ± 899.0	15.8 ± 15.8*	973.2 ± 973.2	1957.8 ± 1131.0	939.2 ± 670.5	Peptidyl-prolyl cis-trans isomerase	Q4S1X7	*Tetraodon nigroviridis*	230	12	2
26		558.7 ± 234.1	377.6 ± 222.6	0.0 ± 0.0*#	0.0 ± 0.0*#	0.0 ± 0.0*#	Uncharacterised protein	A0A0E9WUZ5	*Anguilla anguilla*	62	10	0

Values of protein expression (as determined by spot density) per replicate gel are presented in Table S1 (supplementary information). In general, cAuNPs led to a higher number of proteins with increased abundance whereas PVP-AuNPs led to a higher number of proteins with decreased abundance. Overall, the effects produced on the liver proteome of *S. aurata* of the four tested AuNPs may be ranked as follow: 7 nm cAuNPs>7 nm PVP-AuNPs≈40 nm cAuNPs>40 nm PVP-AuNPs (Figure 4).

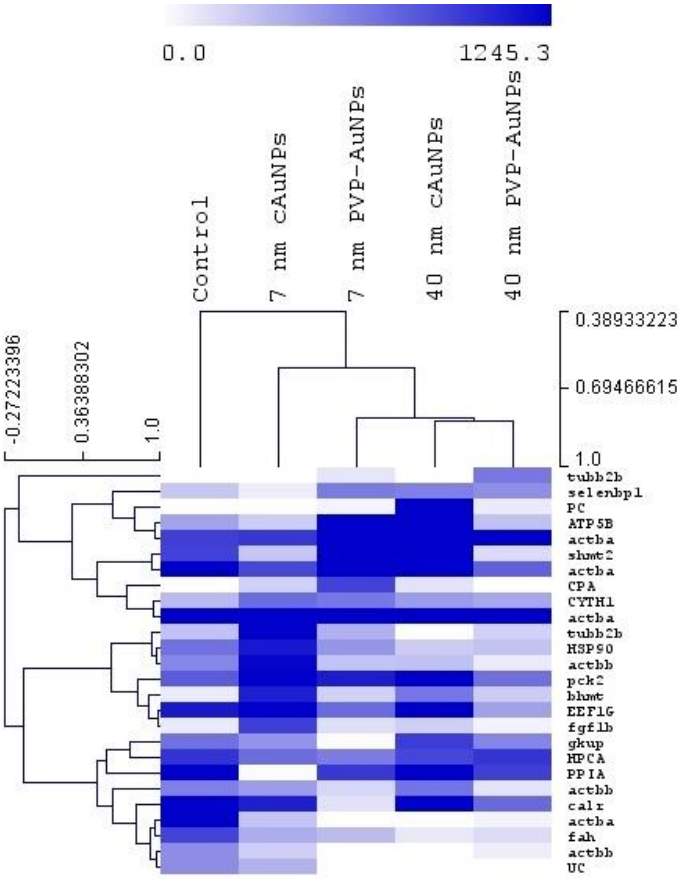

Figure 4. Hierarchical cluster analysis of *Sparus aurata* proteome in response to gold nanoparticles (citrate coated – cAuNPs and polyvinylpyrrolidone coated – PVP-AuNPs). On the vertical axis of the dendrogram: clustering of proteins with similar expression profiles. On the horizontal axis: grouping of samples with similar proteome. Proteins with significant changes in abundance (Dunnett´s test, $p<0.05$) and/or with 3.0-fold changes to control. The abundance of each protein (mean value) is represented in a colour gradient (heat map). UC – Uncharacterised protein.

Bioaccumulation of a chemical is often linked with its toxicity (Loureiro et al. 2018). In the present study, we may say that cAuNPs were more bioactive than PVP-AuNPs despite the greater accumulation of PVP-AuNPs in fish tissues. The number of proteins affected in *S. aurata* liver by cAuNPs was higher in comparison to PVP-AuNPs. A previous study, where different organisms were tested (bacteria, algae, SiHa cell line and mice), also showed that cAuNPs induced more adverse effects than PVP-AuNPs (Iswarya et al. 2016). Wang et al. (2011) reported that the toxicity of AuNPs was related to the co-existence of citrate and Au^{3+} ions. In the absence of reactive citrate ions on the surface of AuNPs coated with PVP, PVP-AuNPs induced less effects than cAuNPs (Iswarya et al. 2016). However, in a previous 96 h exposure study, *S. aurata* hepatic transcriptional response was more pronounced after exposure to 80 $\mu g.L^{-1}$ PVP-AuNPs than 80 $\mu g.L^{-1}$ cAuNPs (Teles et al. 2016). On the one hand, this is an unexpected finding, given that PVP coating is considered safer and more biocompatible than citrate coating (Min et al. 2009). In contrast, the aggregation/agglomeration of cAuNPs in seawater can reduce the presence of these particles in the water column and their bioactivity, whereas the stability of PVP-AuNPs increases their bioavailability in the water to fish (Barreto et al. 2015).

A previous study with Caco-2 cells showed size specific effects of AuNPs on the proteome of these cells, with 5 nm AuNPs inducing differences in abundance in 36 proteins while 30 nm AuNPs inducing differences in 33 (Gioria et al. 2016). It was also described that 88 and 83 proteins displayed differences in abundance in Balb/3T3 mouse fibroblast cell line after exposure to 5 and 15 nm AuNPs,

respectively (Gioria et al. 2014). These studies also support our findings, in that smaller NPs (7 nm) induced more changes in the proteome than larger NPs (40 nm).

Most of the differentially expressed proteins were identified using the UNIPROT database, except for one that could not be identified even after performing a homology search with all protein sequences from the taxonomic class *Actinopterygii*. More information regarding protein identification is shown in the supplementary information (Table S2). Most of the identified proteins were structural (actins and tubulins) as these are among the major constituents and most abundant proteins in tissues and organs, including the liver. As in the present study, abundance of actins was significantly altered after 72 h exposure to 5 and 30 nm AuNPs in Caco-2 cells (Gioria et al. 2016), highlighting that this is a major molecular outcome of the exposure to AuNPs.

In fact, actins were the only common protein target of the four tested AuNPs, while different types of AuNPs affected different metabolic pathways. Several actin isoforms increased or decreased in abundance after the exposure to 7 nm AuNPs (both coatings) and 40 nm cAuNPs and decreased in abundance by 40 nm PVP-AuNPs. In the study of Gioria et al. (2016), in Caco-2 cells, only 33% of the differential spots were found to be common to both treatments (5 and 30 nm AuNPs). In Balb/3T3 cells, among the 111 down-regulated proteins, 25 were common in both treatments (5 and 15 nm AuNPs), while only three were found up-regulated in both treatments, among the 60 up-regulated proteins (Gioria et al. 2014).

Table 5. Molecular function and biological process of proteins displaying differences in abundance in *Sparus aurata* liver after 96 h exposure to gold nanoparticles. Proteins identified with *Danio rerio* and *Actinopterygii* databases. cAuNPs – Citrate coated gold nanoparticles; PVP-AuNPs – Polyvinylpyrrolidone coated gold nanoparticles.

Protein Number	Protein Name	Accession Number	Molecular Function	Biological Process
7 nm cAuNPs				
1	Elongation factor 1-gamma	A0A0F8C4B3	- Elongation factor	- Protein biosynthesis
2	94 kDa glucose-regulated protein	M9NZ74	- ATP binding - Unfolded protein binding	- Protein folding - Response to stress
25	Peptidyl-prolyl cis-trans isomerase	Q4S1X7	- Peptidyl-prolyl cis-trans isomerase activity	- Protein folding
12	Cytohesin-1	A0A146RY54	- ARF guanyl-nucleotide exchange factor activity - Phospholipid binding	- Regulation of ARF protein signal transduction
3	Phosphoenolpyruvate carboxykinase 2 (mitochondrial)	F1R9Y5	- GTP binding - Phosphoenolpyruvate carboxykinase (GTP) activity	- Gluconeogenesis
14	Betaine-homocysteine S-methyltransferase 1	F1QU55	- Betaine-homocysteine S-methyltransferase activity - Zinc ion binding	- Methionine biosynthetic process
22	Fumarylacetoacetate hydrolase (Fumarylacetoacetase)	Q803S0	- Fumarylacetoacetase activity	- Aromatic amino acid family metabolic process
10	Tubulin beta chain	Q32PU7	- GTPase activity - GTP binding - Structural constituent of cytoskeleton	- Microtubule-based process
11	Tubulin beta chain	Q32PU7	- GTPase activity - GTP binding - Structural constituent of cytoskeleton	- Microtubule-based process
16	Actin, cytoplasmic 1	Q7ZVI7	- ATP binding	- Cell structure, cell junction assembly, cell motility, membrane organization
20	Actin, cytoplasmic 2	Q7ZVF9	- ATP binding	- Cell structure, cell junction assembly, cell motility, membrane organization
21	Actin, cytoplasmic 2	Q7ZVF9	- ATP binding	- Cell structure, cell junction assembly, cell motility, membrane organization
24	Fibroblast growth factor	A7YT71	- Fibroblast growth factor receptor binding - Growth factor activity - Heparin binding	- Angiogenesis - Cell differentiation - Fibroblast growth factor receptor signaling pathway - Positive regulation of cell division

Table 5 (continuation). Molecular function and biological process of proteins displaying differences in abundance in *Sparus aurata* liver after 96 h exposure to gold nanoparticles. Proteins identified with *Danio rerio* and *Actinopterygii* databases. cAuNPs – Citrate coated gold nanoparticles; PVP-AuNPs – Polyvinylpyrrolidone coated gold nanoparticles.

Protein Number	Protein Name	Accession Number	Molecular Function	Biological Process
7 nm PVP-AuNPs				
4	Glucuronokinase with putative uridyl pyrophosphorylase	A0A0R4IGN7	- Glucuronokinase activity - Nucleotidyltransferase activity	- Biosynthetic process - Ascorbate metabolism
7	Carboxypeptidase	G3NFY9	- Serine-type carboxypeptidase activity	- Protein catabolism
9	Selenium-binding protein 1	Q6PHD9	- Methanethiol oxidase activity - Selenium binding	- Protein transport
13	Calreticulin	F1Q8W8	- Calcium ion binding - Unfolded protein binding	- Protein folding
15	Actin, cytoplasmic 1	Q7ZVI7	- ATP binding	- Cell structure, cell junction assembly, cell motility, membrane organization
16	Actin, cytoplasmic 1	Q7ZVI7	- ATP binding	- Cell structure, cell junction assembly, cell motility, membrane organization
17	Actin, cytoplasmic 1	Q7ZVI7	- ATP binding	- Cell structure, cell junction assembly, cell motility, membrane organization
18	Actin, cytoplasmic 1	Q7ZVI7	- ATP binding	- Cell structure, cell junction assembly, cell motility, membrane organization
21	Actin, cytoplasmic 2	Q7ZVF9	- ATP binding	- Cell structure, cell junction assembly, cell motility, membrane organization
26	Uncharacterised protein	A0A0E9WUZ5		
40 nm PVP-AuNPs				
6	Mitochondrial serine hydroxymethyltransferase	A9LDD9	- Lycine hydroxymethyltransferase activity - Ethyltransferase activity - Pyridoxal phosphate binding	- Glycine biosynthetic process from serine - Tetrahydrofolate interconversion
22	Fumarylacetoacetate hydrolase (Fumarylacetoacetase)	Q803S0	- Fumarylacetoacetase activity	- Aromatic amino acid family metabolic process
23	Hippocalcin	I3JLG1	- Calcium ion binding	- Cellular response to calcium ion
11	Tubulin beta chain	Q32PU7	- GTPase activity - GTP binding - Structural constituent of cytoskeleton	- Microtubule-based process
16	Actin, cytoplasmic 1	Q7ZVI7	- ATP binding	- Cell structure, cell junction assembly, cell motility, membrane organization
21	Actin, cytoplasmic 2	Q7ZVF9	- ATP binding	- Cell structure, cell junction assembly, cell motility, membrane organization
26	Uncharacterised protein	A0A0E9WUZ5		

Table 5 (continuation). Molecular function and biological process of proteins displaying differences in abundance in *Sparus aurata* liver after 96 h exposure to gold nanoparticles. Proteins identified with *Danio rerio* and *Actinopterygii* databases. cAuNPs – Citrate coated gold nanoparticles; PVP-AuNPs – Polyvinylpyrrolidone coated gold nanoparticles.

Protein Number	Protein Name	Accession Number	Molecular Function	Biological Process
40 nm cAuNPs				
3	Phosphoenolpyruvate carboxykinase 2 (mitochondrial)	F1R9Y5	- GTP binding - Phosphoenolpyruvate carboxykinase (GTP) activity	- Gluconeogenesis
5	ATP synthase subunit beta	A8WGC6	- ATP binding - Proton-transporting ATP synthase activity, rotational mechanism	- ATP synthesis coupled proton transport
8	Pyruvate carboxylase b	B0S5R6	- ATP binding - Metal ion binding - Pyruvate carboxylase activity	- Gluconeogenesis - Pyruvate metabolic process - Response to cadmium ion
9	Selenium-binding protein 1	Q6PHD9	- Methanethiol oxidase activity - Selenium binding	- Protein transport
15	Actin, cytoplasmic 1	Q7ZVI7	- ATP binding	- Cell structure, cell junction assembly, cell motility, membrane organization
16	Actin, cytoplasmic 1	Q7ZVI7	- ATP binding	- Cell structure, cell junction assembly, cell motility, membrane organization
17	Actin, cytoplasmic 1	Q7ZVI7	- ATP binding	- Cell structure, cell junction assembly, cell motility, membrane organization
19	Actin, cytoplasmic 2	Q7ZVF9	- ATP binding	- Cell structure, cell junction assembly, cell motility, membrane organization
21	Actin, cytoplasmic 2	Q7ZVF9	- ATP binding	- Cell structure, cell junction assembly, cell motility, membrane organization
26	Uncharacterised protein	A0A0E9WUZ5		

Actins are abundant cytoskeleton proteins (involved in microfilaments) with an important function in intracellular transport, cell organization and motility processes (Goodson et al. 2002). Therefore, the change in abundance observed in several actin isoforms after AuNPs exposure may be an evidence that liver cells cytoskeleton was affected by NPs. When actins are affected, many cellular mechanisms, ranging from cell motility and the maintenance of cell shape and

polarity to the regulation of transcription can be consequently affected. One of the mechanisms responsible for inducing alterations in actins is oxidative stress, which induces cytoskeleton disorganization (Gomes et al. 2013; Gómez-Mendikute et al. 2003; Rodríguez-Ortega et al. 2003). Tubulins, another key component of the cytoskeleton, that participate in microtubule polymerization, cell transport and motility (Apraiz et al. 2006; Miura et al. 2005), were also altered by 7 nm cAuNPs and 40 nm PVP-AuNPs. In these two treatments, the abundance of tubulins increased, which reinforces our hypothesis that cytoskeleton is one of the main cellular targets of AuNPs. Indeed, alterations in cytoskeletal proteins was already detected in other aquatic organisms exposed to NPs (Gomes et al. 2013, 2014).

Besides the effects in cytoskeletal proteins, the canonical pathway analysis revealed other putative effects of NPs in proteins with functions in gluconeogenesis, amino acids metabolism and protein synthesis, catabolism, folding and transport. The exposure to 7 and 40 nm cAuNPs increased the abundance of proteins involved in gluconeogenesis processes (e.g. phosphoenolpyruvate carboxykinase 2). The “extra” cellular glucose demand may imply their production by noncarbohydrate substrates (e.g., lactate, glycerol and glycogenic amino acids) suggesting a disruption in energetic metabolism. Although proteins are constitutive, their mobilization can occur under stress (such as the exposure to contaminants) (Erk et al. 2011; Maria et al. 2018). Moreover, the abundance of selenium-binding protein, which may be involved in the sensing of reactive xenobiotics in the cytoplasm was increased after the exposure to 7 nm PVP-AuNPs and 40 nm cAuNPs. Cells respond to environmental and physiological stresses through the induction of specific proteins, including 94 kDa glucose-regulated protein, which had its abundance increased after exposure to 7 nm cAuNPs. The abundance of fumarylacetoacetase decreased after the exposure to 7 nm cAuNPs and 40 nm PVP-AuNPs. This enzyme is involved in amino acid catabolism and catalyses the hydrolytic cleavage of fumarylacetoacetate to yield fumarate and acetoacetate as the final step in phenylalanine and tyrosine degradation (Mahanty et al. 2016). Associated with the altered abundance of other enzymes involved in amino acid metabolism (e.g. glucuronokinase with putative uridyl pyrophosphorylase, betaine-homocysteine S-methyltransferase 1 and mitochondrial serine

hydroxymethyltransferase), it seems that AuNPs are compromising primary metabolic processes. As in the present study, after exposure to AuNPs, proteins involved in protein synthesis and amino acid transport were down or up-regulated in Caco-2 cells (Gioria et al. 2016) and proteins such as elongation factor 1-gamma, tubulin, peptidyl-prolyl cis-trans isomerase and ATP synthase displayed differences in abundance in Balb/3T3 cell line (Gioria et al. 2014).

Previous studies showed that 40 nm cAuNPs, at 80 $\mu g.L^{-1}$, increased *S. aurata* hepatic non-protein thiols levels after 96 h exposure (Barreto et al. 2019b) and 40 nm PVP-AuNPs impacted the hepatic expression of antioxidant, immune and apoptosis related genes (Teles et al. 2016). The present data reveal additional/complementary effects of AuNPs potentially impairing the liver metabolism of *S. aurata* which may be linked with the effects previously described.

For more insights on the mechanisms of action of these NPs, we performed a functional protein-interaction analysis using STRING as the bioinformatics tool to retrieve interacting genes/proteins (Figure 5). The analysis included only the differentially expressed proteins for which human homologs could be assigned. The networks displayed in this figure show the functional relationships among the proteins identified in this work, with regard to the four AuNPs tested. Moreover, the analysis shows that several of the differential proteins identified in this study (underlined) are included in numerous of these interacting networks. All networks displayed include different types of proteins, highlighting our previous observations that the presence and accumulation of AuNPs is associated with different molecular responses in fish. The analysis shows, for instance, that phosphoenolpyruvate carboxykinase 2 (PCK2) and peptidyl-prolyl cis-trans isomerase (PPIA) may have a critical role in the action of 7 nm cAuNPs, as these proteins seem to interact, not only with cytoskeletal proteins, but also with a key chaperone (HSP90) and with protein elongation factors (EEF), which play important roles in the regulation of protein transcription. Moreover calreticulin (CALR), identified in this study, may have increased importance in the bioactivity of 7 nm PVP-AuNPs since this protein seems to interact and alongside may play a role in the regulation of different proteins including chaperones (HSP90, HSPA5) and cytoskeletal proteins (ACTB, ACTG1). The bioactivity of 40 nm cAuNPs is likely linked to PCK2, PC and ATP5B. These

proteins seem to be functionally related, and changes in these proteins will likely have strong implications in the synthesis of ATP of which many cellular processes depend including cytoskeletal proteins (ACTG1, ACTB). Finally, the proteins fumarylacetoacetase (FAH) and serine hydroxymethyltransferase (SHMT2) seem to participate in other mechanisms of bioactivity of 40 nm PVP-AuNPs.

7 nm cAuNPs

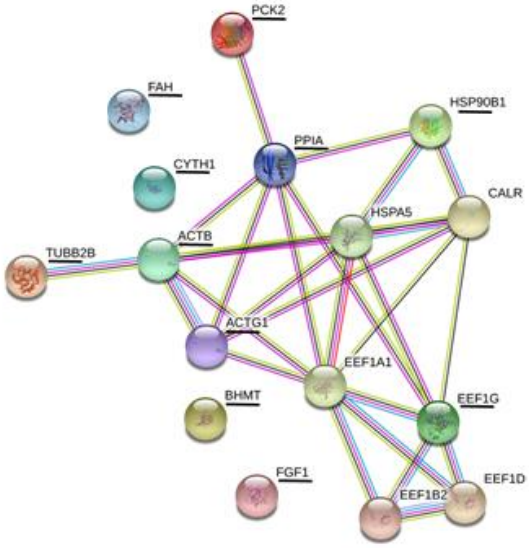

7 nm PVP-AuNPs

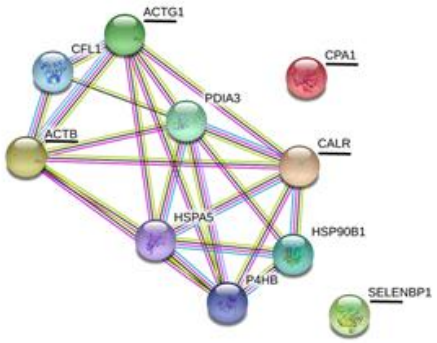

40 nm cAuNPs

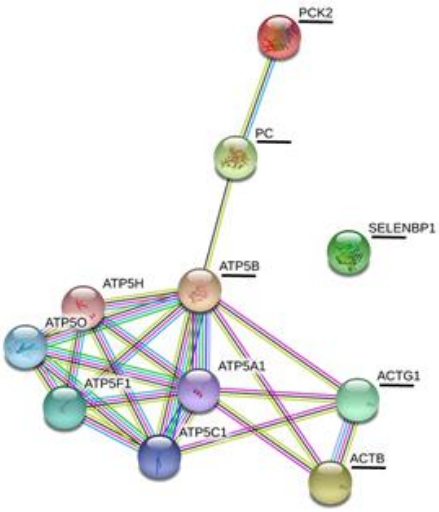

40 nm PVP-AuNPs

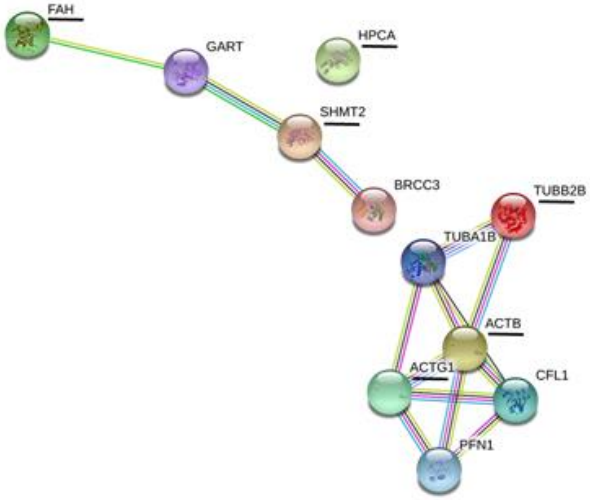

Figure 5. Predicted protein functional associations, from STRING database analysis. Proteins identified in this work are underlined whereas other proteins displayed in the network are potential interactors predicted by the program. The evidences supporting these associations come from different sources (curated databases, experimentally determined, gene neighbourhood, gene fusions, gene co-occurrence, text mining, co-expression, protein homology) and are represented by edges of different colours (for detailed legend of the edges, consult the program page https://string-db.org/). Proteins linked by edges are functionally related and several proteins can form more or less complex interacting networks.

4. Conclusions

The present work revealed proteomic changes in *S. aurata* liver after the exposure to different AuNPs. From analysis of 2-DE gels, 26 proteins, mainly involved in cytoskeleton and cell structure, gluconeogenesis, amino acids metabolism and other metabolic processes (e.g. regulation of protein activity), showed differences in abundance (down or up-regulation) after the exposure to different AuNPs. Additionally, the abundance of proteins involved in stress response was increased after the exposure to AuNPs. The effects were dependent on AuNPs characteristics, with cAuNPs inducing more effects in the proteome of *S. aurata* than PVP-AuNPs. Despite gold accumulating more in the tissues of *S. aurata* after exposure to 7 nm PVP-AuNPs, including liver, 7 nm cAuNPs induced greater effects in the fish liver proteome than the other tested AuNPs. cAuNPs were more bioactive than PVP-AuNPs and due to this we speculate that cAuNPs may be more toxic than PVP-AuNPs. The highest accumulation of gold found in the spleen of fish comparing with the other tissues is also an important finding, supporting the need for further studies. Overall, we may state that proteomics was a sensitive approach to identify effects of AuNPs, at sub-lethal concentrations, on the metabolism of *S. aurata*, and to raise hypothesis concerning the mechanisms of action of AuNPs and their putative toxicity. Additionally, the proteomics approach allowed to differentiate responses of AuNPs differing in size and coating.

Conflict of interest statement

The authors declare that there are no conflicts of interest.

Acknowledgments

Thanks are due for the financial support to CESAM (UID/AMB/50017/2019), to FCT/MCTES through national funds, and the co-funding by the FEDER, within the PT2020 Partnership Agreement and Compete 2020. This research was supported through the COMPETE – Operational Competitiveness Program and national funds through FCT, under the project “NANOAu – Effects of Gold Nanoparticles to Aquatic Organisms” (FCT PTDC/MAR-EST/3399/2012) (FCOMP-01-0124-FEDER-029435), through FCT/MCTES through national funds (PIDDAC), the cofounding by FEDER, within the PT2020 Partnership Agreement and Compete 2020. A. Barreto has a doctoral fellowship from FCT (SFRH/BD/97624/2013). M. Oliveira has financial support of the program Investigator FCT, co-funded by the Human Potential Operational Programme and European Social Fund (IF/00335(2015)). The mass spectrometry technique was performed at the Proteomics i3S Scientific Platform with the assistance of H. Osório. This work had support from the Portuguese Mass Spectrometry Network, integrated in the National Roadmap of Research Infrastructures of Strategic Relevance (ROTEIRO/0028/2013; LISBOA-01-0145-FEDER-022125). This work was also partially funded by the project UID/Multi/04423/2019 funded by FCT.

5. References

Alves, R. N., O. Cordeiro, T. S. Silva, N. Richard, M. de Vareilles, G. Marino, P. Di Marco, P. M. Rodrigues, and L. E. C. Conceição. 2010. 'Metabolic molecular indicators of chronic stress in gilthead seabream (*Sparus aurata*) using comparative proteomics', *Aquaculture*, 299: 57-66.

Apraiz, I., J. Mi, and S. Cristobal. 2006. 'Identification of proteomic signatures of exposure to marine pollutants inmussels (*Mytilus edulis*)', *Molecular & Cellular Proteomics*, 5: 1274-85.

Bajak, E., M. Fabbri, J. Ponti, S. Gioria, I. Ojea-Jiménez, A. Collotta, V. Mariani, D. Gilliland, F. Rossi, and L. Gribaldo. 2015. ‘Changes in Caco-2 cells transcriptome profiles upon exposure to gold nanoparticles’, *Toxicology Letters,* 233: 187-99.

Barreto, A., L. G. Luis, A. V. Girão, T. Trindade, A. M. V. M. Soares, and M. Oliveira. 2015. 'Behavior of colloidal gold nanoparticles in different ionic strength media', *Journal of Nanoparticle Research*, 17: 1-13.

Barreto, A., L. G. Luis, E. Pinto, A. Almeida, P. Paíga , L. H. M. L. M. Santos, C. Delerue-Matos, T. Trindade, A. M. V. M. Soares, K. Hylland, S. Loureiro, M. Oliveira. 2019a. 'Genotoxicity of gold nanoparticles in the gilthead seabream (*Sparus aurata*) after single exposure and combined with the pharmaceutical gemfibrozil', *Chemosphere*, 220:11-19.

Barreto, A., L. G. Luis, E. Pinto, A. Almeida, P. Paíga , L. H. M. L. M. Santos, C. Delerue-Matos, T. Trindade, A. M. V. M. Soares, K. Hylland, S. Loureiro, M. Oliveira. 2019b. 'Effects and bioaccumulation of gold nanoparticles in the gilthead seabream (*Sparus aurata*) – Single and combined exposures with gemfibrozil', *Chemosphere*, 215:248-60.

Botha, T. L., T. E. James, and V. Wepener. 2015. 'Comparative Aquatic Toxicity of Gold Nanoparticles and Ionic Gold Using a Species Sensitivity Distribution Approach', *Journal of Nanomaterials*, 2015: 986902.

Bradford, M. M. 1976. 'A rapid and sensitive method for the quantitation of microgram quantities of protein utilizing the principle of protein-dye binding', *Analytical Biochemistry*, 72: 248-54.

Campos, A., M. Puerto, A. Prieto, A. Camean, A. M. Almeida, A. V. Coelho, and V. Vasconcelos. 2013. 'Protein extraction and two-dimensional gel electrophoresis of proteins in the marine mussel *Mytilus galloprovincialis*: an important tool for protein expression studies, food quality and safety assessment', *Journal of the Science of Food and Agriculture*, 93: 1779-87.

Chen, H., A. Dorrigan, S. Saad, D. J. Hare, M. B. Cortie, and S. M. Valenzuela. 2013. '*In vivo* study of spherical gold nanoparticles: inflammatory effects and distribution in mice', *Plos One*, 8: e58208.

Chen Y. S. , Y. C. Hung, I. Liau, G. S. Huang. 2009. 'Assessment of the in vivo toxicity of gold nanoparticles'. *Nanoscale Research Letters*, 4: 85864.

Cordero, H., P. Morcillo, A. Cuesta, M. F. Brinchmann, and M. A. Esteban. 2016. 'Differential proteome profile of skin mucus of gilthead seabream (*Sparus aurata*) after probiotic intake and/or overcrowding stress', *Journal of Proteomics*, 132: 41-50.

Coles, J. A., S. R. Farley, R. K. Pipe, 1995. 'Alteration of the immune response of the common marine mussel *Mytilus edulis* resulting from exposure to cadmium', *Diseases of Aquatic Organisms*, 22: 59-65.

Dedeh, A., A. Ciutat, M. Treguer-Delapierre, and J.-P. Bourdineaud. 2015. 'Impact of gold nanoparticles on zebrafish exposed to a spiked sediment', *Nanotoxicology*, 9: 71-80.

Dhumale, V. A., R. K. Gangwar, K. Rajesh, S. S. Datar, R. B. Sharma. 2012. 'Reversible Aggregation Control of Polyvinylpyrrolidone Capped Gold Nanoparticles as a Function of pH', *Materials Express*, 2: 311-18.

Erk, M., D. Ivankovic, and Z. Strizak. 2011. 'Cellular energy allocation in mussels (*Mytilus galloprovincialis*) from the stratified estuary as a physiological biomarker', *Marine Pollution Bulletin*, 62: 1124-29.

Ferreira, P., E. Fonte, M. E. Soares, F. Carvalho, L. Guilhermino. 2016. 'Effects of multi-stressors on juveniles of the marine fish *Pomatoschistus microps*: gold nanoparticles, microplastics and temperature', *Aquatic Toxicology*, 170: 89-103.

García-Cambero, J. P., M. N. García, G. D. López, A. L. Herranz, L. Cuevas, E. Pérez-Pastrana, J. S. Cuadal, M. R. Castelltort, and A. C. Calvo. 2013. 'Converging hazard assessment of gold nanoparticles to aquatic organisms', *Chemosphere*, 93: 1194-200.

García-Negrete, C. A., J. Blasco, M. Volland, T. C. Rojas, M. Hampel, A. Lapresta-Fernández, M. C. Jiménez de Haro, M. Soto, and A. Fernández. 2013. 'Behaviour of Au-citrate nanoparticles in seawater and accumulation in bivalves at environmentally relevant concentrations', *Environmental Pollution*, 174: 134-41.

Ghisaura, S., R. Anedda, D. Pagnozzi, G. Biosa, S. Spada, E. Bonaglini, R. Cappuccinelli, T. Roggio, S. Uzzau, and M. F. Addis. 2014. 'Impact of three commercial feed formulations on farmed gilthead sea bream (*Sparus aurata*, L.) metabolism as inferred from liver and blood serum proteomics', *Proteome Science*, 12: 44.

Gioria, S., H. Chassaigne, D. Carpi, A. Parracino, S. Meschini, P. Barboro, and F. Rossi. 2014. 'A proteomic approach to investigate AuNPs effects in Balb/3T3 cells', *Toxicology Letters*, 228: 111-26.

Gioria, S., J. L. Vicente, P. Barboro, R. La Spina, G. Tomasi, P. Urban, A. Kinsner-Ovaskainen, R. Francois, and H. Chassaigne. 2016. 'A combined proteomics and metabolomics approach to assess the effects of gold nanoparticles *in vitro*', *Nanotoxicology*, 10: 736-48.

Gobom, J., E. Nordhoff, E. Mirgorodskaya, R. Ekman, and P. Roepstorff. 1999. ‘Sample purification and preparation technique based on nano-scale reversed-phase columns for the sensitive analysis of complex peptide mixtures by matrix-assisted laser desorption/ionization mass spectrometry’, *Journal of Mass Spectrometry*, 34: 105-16.

Goodson, H. V., and W. F. Hawse. 2002. ‘Molecular evolution of the actin family‘, *Journal of Cell Science*, 115: 2619-22.

Gomes, T., C. G. Pereira, C. Cardoso, and M. J. Bebianno. 2013. ‘Differential protein expression in mussels *Mytilus galloprovincialis* exposed to nano and ionic Ag‘, *Aquatic Toxicology*, 136-137: 79-90.

Gomes, T., S. Chora, C. G. Pereira, C. Cardoso, and M. J. Bebianno. 2014. ‘Proteomic response of mussels *Mytilus galloprovincialis* exposed to CuO NPs and Cu^{2+}: An exploratory biomarker discovery‘, *Aquatic Toxicology*, 155: 327-36.

Gómez-Mendikute, A., and M. P. Cajaraville. 2003. ‘Comparative effects of cadmium, copper, paraquat and benzo[a]pyrene on the actin cytoskeleton and production of reactive oxygen species (ROS) in mussel haemocytes‘, *Toxicology in Vitro*, 17: 539-46.

Gupta, Y. R., D. Sellegounder, M. Kannan, S. Deepa, B. Senthilkumaran, and Y. Basavaraju. 2016. ‘Effect of copper nanoparticles exposure in the physiology of the common carp (*Cyprinus carpio*): Biochemical, histological and proteomic approaches’, *Aquaculture and Fisheries*, 1: 15-23.

Hanžić, N., T. Jurkin, A. Maksimović, and M. Gotić. 2015. 'The synthesis of gold nanoparticles by a citrate-radiolytical method', *Radiation Physics and Chemistry*, 106: 77-82.

Huang, K., H. Ma, J. Liu, S. Huo, A. Kumar, T. Wei, X. Zhang, S. Jin, Y. Gan, P. C. Wang, S. He, X. Zhang, and X.-J. Liang. 2012. ‘Size-Dependent Localization and Penetration of Ultrasmall Gold Nanoparticles in Cancer Cells, Multicellular Spheroids, and Tumors *in Vivo*’, *ACS Nano*, 6: 4483-93.

Iswarya, V., J. Manivannan, A. De, S. Paul, R. Roy, J. B. Johnson, R. Kundu, N. Chandrasekaran, A. Mukherjee, and A. Mukherjee. 2016. 'Surface capping and size-dependent toxicity of gold nanoparticles on different trophic levels', *Environmental Science and Pollution Research*, 23: 4844-58.

Khan, M. S., G. D. Vishakante, and H. Siddaramaiah. 2013. 'Gold nanoparticles: A paradigm shift in biomedical applications', *Advances in Colloid and Interface Science*, 199-200: 44-58.

Khanna, P., C. Ong, B. Bay, and G. Baeg. 2015. 'Nanotoxicity: An Interplay of Oxidative Stress, Inflammation and Cell Death', *Nanomaterials*, 5: 1163.

Kondera, E., K. Ługowska, and P. Sarnowski. 2014. 'High affinity of cadmium and copper to head kidney of common carp (*Cyprinus carpio* L.)', *Fish Physiology and Biochemistry*, 40: 9-22.

Lee, B., C. N. Duong, J. Cho, J. Lee, K. Kim, Y. Seo, P. Kim, K. Choi, J. Yoon. 2012. 'Toxicity of citrate-capped silver nanoparticles in common carp (*Cyprinus carpio*)', *Journal of Biomedicine and Biotechnology*, 2012: 262670.

Lekeufack, D. Djoumessi, A. Brioude, A. Mouti, J. G. Alauzun, P. Stadelmann, A. W. Coleman, and P. Miele. 2010. 'Core-shell Au@(TiO_2, SiO_2) nanoparticles with tunable morphology', *Chemical Communications*, 46: 4544-46.

Li, C., D. Li, G. Wan, J. Xu, and W. Hou. 2011. 'Facile synthesis of concentrated gold nanoparticles with low size-distribution in water: temperature and pH controls', *Nanoscale Research Letters*, 6: 1-10.

Loureiro, S., P. Tourinho, G. Cornelis, N. Van Den Brink, M. Díez-Ortiz, S. Vázquez-Campos, V. Pomar-Portillo, C. Svendsen, and C. A. M. Van Gestel. 2018. Chapter 7: Nanomaterials as Soil Pollutants. In book: Soil Pollution. 161-90.Matysiak, M., L. Kapka-Skrzypczak, K. Brzóska, A. C. Gutleb, and M.Kruszewski. 2016. 'Proteomic approach to nanotoxicity', *Journal of Proteomics*, 137: 35-44.

Mahanty, A., G. K. Purohit, S. Banerjee, D. Karunakaran, S. Mohanty, and B. P. Mohanty. 2016. 'Proteomic changes in the liver of *Channa striatus* in response to high temperature stress'. *Electrophoresis*, 37: 1704-17.

Maria, V. L., D. Licha, J. J. Scott-Fordsmand, C. G. Huber, and M. J. B. Amorim. 2018. 'The Proteome of *Enchytraeus crypticus* – Exposure to CuO Nanomaterial and $CuCl_2$ – in Pursue of a Mechanistic Interpretation'. *Proteomics*, 18: 1800091.

Mateo, D., P. Morales, A. Ávalos, and A. Haza. 2014. 'Oxidative stress contributes to gold nanoparticle-induced cytotoxicity in human tumor cells'. *Toxicology Mechanisms and Methods*, 24: 161-72.

Min, Z., W. Baoxiang, R. Zbigniew, X. Zhaohui, F. J. Otto, Y. Xiaofeng, and R. Steinar. 2009. 'Minute synthesis of extremely stable gold nanoparticles', *Nanotechnology*, 20: 505606.

Mirzajani, F., H. Askari, S. Hamzelou, Y. Schober, A. Römpp, A. Ghassempour, and B. Spengler. 2014a. 'Proteomics study of silver nanoparticles toxicity on *Bacillus thuringiensis'*, *Ecotoxicology and Environmental Safety*, 100: 122-30.

Mirzajani, F., H. Askari, S. Hamzelou, Y. Schober, A. Römpp, A. Ghassempour, and B. Spengler. 2014b. 'Proteomics study of silver nanoparticles toxicity on *Oryza sativa* L.', *Ecotoxicology and Environmental Safety*, 108: 335-39.

Miura, Y., M. Kano, K. Abe, S. Urano, S. Suzuki, and T. Toda. 2005. 'Age-dependent variations of cell response to oxidative stress: proteomic approach to protein expression and phosphorylation', *Electrophoresis*, 26: 2786-96.

Naderi, M., S. Keyvanshokooh, A.P. Salati, and A. Ghaedi. 2017. ‘Proteomic analysis of liver tissue from rainbow trout (*Oncorhynchus mykiss*) under high rearing density after administration of dietary vitamin E and selenium nanoparticles’, *Comparative Biochemistry and Physiology Part D Genomics Proteomics*, 22: 10-19.

NIST. 2010. 'NCL method PCC-8, determination of gold in rat tissue with inductively coupled plasma mass spectrometry'.

OECD. 1992. *Test No. 203: fish, acute toxicity test* (OECD Publishing).

Osório, H., A. M. Almeida, and A. Campos. 2017. Sample Preparation for 2DE Using Samples of Animal Origin. *In*: Proteomics in Domestic Animals: from Farm to Systems Biology. de Almeida AM, Eckersall D, Miller I (Eds.). Springer International Publishing AG.

Otelea, M., and A. Rascu. 2015. 'Genomics and proteomics techniques in nanoparticles studies – New approach in environmental research'. *Environmental engineering and management journal*, 14: 2283-91.

Piotrowska, G. B., J. Golimowski, and P. L. Urban. 2009. 'Nanoparticles: Their potential toxicity, waste and environmental management'. *Waste Management*, 29: 2587-95.

Pandey, A., and M. Mann. 2000. 'Proteomics to study genes and genomes', *Nature*, 405: 837-46.

Planchon, M., T. Léger, O. Spalla, G. Huber, and R. Ferrari. 2017. 'Metabolomic and proteomic investigations of impacts of titanium dioxide nanoparticles on *Escherichia coli*', *Plos One*, 12: e0178437.

Rodríguez-Ortega, M. J., B. E. Grøsvik, A. Rodríguez-Ariza, A. Goksøyr, J. López-Barea. 2003. 'Changes in protein expression profiles in bivalve molluscs (*Chamaelea gallina*) exposed to four model environmental pollutants', *Proteomics*, 3: 1535-43.

Rønneseth, A., H. I. Wergeland, and E. F. Pettersen. 2007. 'Neutrophils and B-cells in Atlantic cod (*Gadus morhua* L.)', *Fish & Shellfish Immunology*, 23: 493-503.

Rufino-Palomares, E., F. J. Reyes-Zurita, C. A. Fuentes-Almagro, M. de la Higuera, J. A. Lupianez, and J. Peragon. 2011. 'Proteomics in the liver of gilthead sea bream (*Sparus aurata*) to elucidate the cellular response induced by the intake of maslinic acid', *Proteomics*, 11: 3312-25.

Shiba, F. 2013. 'Size control of monodisperse Au nanoparticles synthesized via a citrate reduction process associated with a pH-shifting procedure', *CrystEngComm*, 15: 8412-15.

Simpson, C. A., K. J. Salleng, D. E. Cliffel, and D. L. Feldheim. 2013. '*In vivo* toxicity, biodistribution, and clearance of glutathione-coated gold nanoparticles', *Nanomedicine: Nanotechnology, Biology and Medicine*, 9: 257-63.

Tedesco, S., H. Doyle, J. Blasco, G. Redmond, and D. Sheehan. 2010. 'Oxidative stress and toxicity of gold nanoparticles in *Mytilus edulis*', *Aquatic Toxicology*, 100: 178-86.

Teles, M., C. Fierro-Castro, P. Na-Phatthalung, A. Tvarijonaviciute, T. Trindade, A. M. V. M. Soares, L. Tort, and M. Oliveira. 2016. 'Assessment of gold nanoparticle

effects in a marine teleost (*Sparus aurata*) using molecular and biochemical biomarkers', *Aquatic Toxicology*, 177: 125-35.

Tiede, K., M. Hassellöv, E. Breitbarth, Q. Chaudhry, and A. B. A. Boxall. 2009. 'Considerations for environmental fate and ecotoxicity testing to support environmental risk assessments for engineered nanoparticles', *Journal of Chromatography A*, 1216: 503-09.

Turkevich, J., P. C. Stevenson, and J. Hillier. 1951. 'A study of the nucleation and growth processes in the synthesis of colloidal gold', *Discussions of the Faraday Society*, 11: 55-75.

Vale, G., K. Mehennaoui, S. Cambier, G. Libralato, S. Jomini, and R. F. Domingos. 2016. 'Manufactured nanoparticles in the aquatic environment-biochemical responses on freshwater organisms: A critical overview', *Aquatic Toxicology*, 170: 162-74.

Varo, I., G. Rigos, J. C. Navarro, J. del Ramo, J. Calduch-Giner, A. Hernandez, J. Pertusa, and A. Torreblanca. 2010. ‘Effect of ivermectin on the liver of gilthead sea bream *Sparus aurata*: a proteomic approach’, *Chemosphere*, 80: 570–77.

Volker, N., A. Norbert, T. Dieter, and E. Wolfgang. 1988. 'Improved staining of proteins in polyacrylamide gels including isoelectric focusing gels with clear background at nanogram sensitivity using Coomassie Brilliant Blue G-250 and R-250', *Electrophoresis*, 9: 255-62.

Yoo-Iam, M., R. Chaichana, and T. Satapanajaru. 2014. 'Toxicity, bioaccumulation and biomagnification of silver nanoparticles in green algae (*Chlorella* sp.), water flea (*Moina macrocopa*), blood worm (*Chironomus* spp.) and silver barb (*Barbonymus gonionotus*)', *Chemical Speciation and Bioavailability*, 26: 257-65.

Wang, S., R. Lawson, P.C. Ray, H. Yu. 2011. 'Toxic effects of gold nanoparticles on *Salmonella typhimurium* bacteria', *Toxicology and Industrial Health*, 27: 547-54.

Zeng, S., M. Cai, H. Liang, and J. Hao. 2012. 'Size-dependent colorimetric visual detection of melamine in milk at 10 ppb level by citrate-stabilized Au nanoparticles', *Analytical Methods*, 4: 2499-505.

Supplementary Information

Table S1. Proteins displaying differences in abundance in *Sparus aurata* liver after 96 h exposure to gold nanoparticles (citrate coated – cAuNPs and polyvinylpyrrolidone coated – PVP-AuNPs), assessed by 2-DE. Values of protein expression are presented as spot density per gel replica and mean spot density of the four gels ± standard error (SD).

		Protein Expression				
Protein Number		**Control**	**7 nm cAuNPs**	**7 nm PVP-AuNPs**	**40 nm cAuNPs**	**40 nm PVP-AuNPs**
1	Gel 1	854.9	1928.0	1658.8	1772.2	0.0
	Gel 2	569.5	2874.3	452.2	951.6	706.6
	Gel 3	2276.0	6940.6	0.0	1725.3	0.0
	Gel 4	816.8	0.0	793.9	551.9	1131.8
	Mean ± SD	**1129.3 ± 287.4**	**2935.7 ± 1462.8***	**726.2 ± 350.8**	**1250.3 ± 299.3**	**459.6 ± 279.2**
2	Gel 1	845.3	978.0	1160.1	868.4	392.6
	Gel 2	471.9	0.0	915.0	0.0	559.6
	Gel 3	1184.5	3538.5	0.0	0.0	0.0
	Gel 4	277.5	0.0	0.0	149.2	227.7
	Mean ± SD	**694.8 ± 201.3**	**1129.1 ± 835.6***	**518.8 ± 303.7**	**254.4 ± 207.7**	**295.0 ± 119.4**
3	Gel 1	939.0	1022.5	2545.3	3667.4	861.5
	Gel 2	1262.7	1118.2	1894.9	3013.1	1116.9
	Gel 3	273.7	1850.3	0.0	726.9	575.1
	Gel 4	744.7	3441.5	0.0	0.0	277.5
	Mean ± SD	**805.0 ± 206.8**	**1858.1 ± 559.2***	**1110.1 ± 654.5**	**1851.8 ± 882.2***	**707.7 ± 181.1**
4	Gel 1	1496.8	779.7	40.7	1912.9	0.0
	Gel 2	232.9	0.0	0.0	588.9	504.3
	Gel 3	1051.0	670.5	0.0	0.0	1871.8
	Gel 4	0.0	650.5	0.0	1318.7	0.0
	Mean ± SD	**695.2 ± 349.5**	**525.2 ± 177.3**	**10.2 ± 10.2***	**955.1 ± 417.9**	**594.0 ± 442.2**

Table S1 (continuation). Proteins displaying differences in abundance in Sparus aurata liver after 96 h exposure to gold nanoparticles (citrate coated – cAuNPs and polyvinylpyrrolidone coated – PVP-AuNPs), assessed by 2-DE. Values of protein expression are presented as spot density per gel replica and mean spot density of the four gels ± standard error (SD).

		Protein Expression				
Protein Number		**Control**	**7 nm cAuNPs**	**7 nm PVP-AuNPs**	**40 nm cAuNPs**	**40 nm PVP-AuNPs**
5	Gel 1	444.6	397.8	1124.4	778.3	0.0
	Gel 2	553.8	0.0	0.0	2542.7	649.8
	Gel 3	807.1	0.0	3585.0	4906.7	0.0
	Gel 4	0.0	592.7	455.3	0.0	558.9
	Mean ± SD	**451.4 ± 168.5**	**247.6 ± 148.4**	**1291.2 ± 798.7**	**2056.9 ± 1088.7***	**302.2 ± 175.5**
6	Gel 1	1106.9	0.0	0.0	1791.9	0.0
	Gel 2	1106.6	0.0	2128.3	1804.3	0.0
	Gel 3	1492.5	0.0	4434.9	1384.8	0.0
	Gel 4	0.0	1108.5	0.0	0.0	307.7
	Mean ± SD	**926.5 ± 321.9**	**277.1 ± 277.1**	**1640.8 ± 1057.9**	**1245.3 ± 426.4**	**76.9 ± 76.9***
7	Gel 1	0.0	0.0	1029.7	0.0	0.0
	Gel 2	0.0	0.0	1217.8	542.2	0.0
	Gel 3	0.0	0.0	1447.4	0.0	0.0
	Gel 4	0.0	905.4	0.0	0.0	0.0
	Mean ± SD	**0.0 ± 0.0**	**226.4 ± 226.4**	**923.7 ± 319.5*#**	**135.5 ± 135.5**	**0.0 ± 0.0**
8	Gel 1	0.0	0.0	0.0	0.0	401.6
	Gel 2	0.0	0.0	0.0	0.0	0.0
	Gel 3	0.0	0.0	202.5	469.3	0.0
	Gel 4	0.0	0.0	0.0	0.0	0.0
	Mean ± SD	**0.0 ± 0.0**	**0.0 ± 0.0**	**50.6 ± 50.6**	**117.3 ± 117.3*#**	**100.4 ± 100.4**

Table S1 (continuation). Proteins displaying differences in abundance in Sparus aurata liver after 96 h exposure to gold nanoparticles (citrate coated – cAuNPs and polyvinylpyrrolidone coated – PVP-AuNPs), assessed by 2-DE. Values of protein expression are presented as spot density per gel replica and mean spot density of the four gels ± standard error (SD).

		Protein Expression				
Protein Number		**Control**	**7 nm cAuNPs**	**7 nm PVP-AuNPs**	**40 nm cAuNPs**	**40 nm PVP-AuNPs**
9	Gel 1	523.1	352.4	892.1	1871.6	801.5
	Gel 2	239.8	0.0	1686.8	613.6	636.1
	Gel 3	0.0	0.0	0.0	0.0	533.2
	Gel 4	347.8	0.0	0.0	0.0	228.1
	Mean ± SD	**277.7 ± 109.4**	**88.1 ± 88.1**	**644.7 ± 406.0***	**621.2 ± 441.2***	**549.7 ± 120.6**
10	Gel 1	0.0	0.0	957.9	0.0	731.9
	Gel 2	0.0	2063.7	946.5	0.0	0.0
	Gel 3	1190.2	1620.7	576.1	0.0	0.0
	Gel 4	0.0	1354.1	0.0	0.0	154.7
	Mean ± SD	**297.6 ± 297.6**	**1259.6 ± 444.7***	**383.5 ± 224.9**	**0.0 ± 0.0**	**221.6 ± 173.9**
11	Gel 1	0.0	0.0	0.0	0.0	1477.6
	Gel 2	0.0	0.0	507.1	0.0	333.0
	Gel 3	0.0	0.0	0.0	0.0	845.2
	Gel 4	0.0	0.0	0.0	0.0	0.0
	Mean ± SD	**0.0 ± 0.0**	**0.0 ± 0.0**	**126.8 ± 126.8**	**0.0 ± 0.0**	**664.0 ± 322.1*#**
12	Gel 1	508.6	818.2	683.5	1230.6	0.0
	Gel 2	0.0	0.0	0.0	627.9	666.0
	Gel 3	421.8	2060.6	1483.1	0.0	870.7
	Gel 4	431.6	0.0	478.3	82.7	198.3
	Mean ± SD	**340.5 ± 115.2**	**719.7 ± 486.8***	**661.2 ± 309.1**	**485.3 ± 284.8**	**433.8 ± 201.7**

Table S1 (continuation). Proteins displaying differences in abundance in Sparus aurata liver after 96 h exposure to gold nanoparticles (citrate coated – cAuNPs and polyvinylpyrrolidone coated – PVP-AuNPs), assessed by 2-DE. Values of protein expression are presented as spot density per gel replica and mean spot density of the four gels ± standard error (SD).

		Protein Expression				
Protein Number		**Control**	**7 nm cAuNPs**	**7 nm PVP-AuNPs**	**40 nm cAuNPs**	**40 nm PVP-AuNPs**
13	Gel 1	6539.4	401.3	0.0	3178.5	0.0
	Gel 2	2812.1	1221.4	0.0	2059.8	1955.5
	Gel 3	3346.1	2401.1	569.3	1547.9	978.4
	Gel 4	0.0	374.2	0.0	0.0	0.0
	Mean ± SD	**3174.4 ± 1340.4**	**1099.5 ± 476.3**	**142.3 ± 142.3***	**1696.5 ± 660.1**	**733.5 ± 468.1**
14	Gel 1	404.1	1176.5	895.0	868.3	404.7
	Gel 2	0.0	0.0	0.0	553.4	0.0
	Gel 3	0.0	1523.4	0.0	1242.5	598.8
	Gel 4	0.0	1701.5	0.0	0.0	0.0
	Mean ± SD	**101.0 ± 101.0**	**1100.4 ± 382.7***	**223.8 ± 223.8**	**666.1 ± 262.3**	**250.9 ± 150.2**
15	Gel 1	1533.6	972.8	2170.5	6021.1	613.9
	Gel 2	0.0	0.0	2834.0	734.5	720.6
	Gel 3	170.8	2638.2	10107.9	0.0	1764.7
	Gel 4	0.0	0.0	631.4	980.0	0.0
	Mean ± SD	**426.1 ± 371.4**	**902.7 ± 662.3**	**3935.9 ± 2108.4***	**1933.9 ± 1378.2***	**774.8 ± 366.2**
16	Gel 1	522.1	0.0	0.0	0.0	0.0
	Gel 2	297.1	1142.1	0.0	0.0	232.4
	Gel 3	10358.3	0.0	0.0	0.0	0.0
	Gel 4	0.0	0.0	0.0	0.0	0.0
	Mean ± SD	**2794.4 ± 2523.6**	**285.5 ± 285.5***	**0.0 ± 0.0***	**0.0 ± 0.0***	**58.1 ± 58.1***

Table S1 (continuation). Proteins displaying differences in abundance in Sparus aurata liver after 96 h exposure to gold nanoparticles (citrate coated – cAuNPs and polyvinylpyrrolidone coated – PVP-AuNPs), assessed by 2-DE. Values of protein expression are presented as spot density per gel replica and mean spot density of the four gels ± standard error (SD).

		Protein Expression				
Protein Number		**Control**	**7 nm cAuNPs**	**7 nm PVP-AuNPs**	**40 nm cAuNPs**	**40 nm PVP-AuNPs**
17	Gel 1	1013.9	1706.4	2644.7	2216.7	0.0
	Gel 2	0.0	2212.8	2258.6	3822.3	967.7
	Gel 3	2585.0	0.0	9352.1	10535.8	5271.1
	Gel 4	155.8	0.0	921.4	912.4	0.0
	Mean ± SD	**938.7 ± 592.3**	**979.8 ± 575.1**	**3794.2 ± 1889.1***	**4371.8 ± 2139.1***	**1559.7 ± 1258.0**
18	Gel 1	5858.8	3539.4	10389.1	6944.1	1218.56
	Gel 2	807.1	11996.8	6854.6	2837.8	2404.26
	Gel 3	3017.0	1014.2	7095.1	6260.2	3071.35
	Gel 4	280.6	6447.2	0.0	118.2	2409.23
	Mean ± SD	**2490.9 ± 1259.5**	**5749.4 ± 2359.8**	**6084.7 ± 2182.6***	**4040.1 ± 1586.1**	**2275.9 ± 385.7**
19	Gel 1	628.8	705.6	0.0	2730.3	520.2
	Gel 2	637.5	0.0	0.0	0.0	0.0
	Gel 3	444.7	0.0	783.1	0.0	0.0
	Gel 4	780.1	1240.8	0.0	0.0	0.0
	Mean ± SD	**622.8 ± 68.7**	**486.6 ± 301.4**	**195.8 ± 195.8**	**682.6 ± 682.6***	**130.0 ± 130.0**
20	Gel 1	1144.4	0.0	1170.9	1193.1	408.4
	Gel 2	730.1	4254.9	0.0	0.0	0.0
	Gel 3	0.0	659.0	0.0	0.0	0.0
	Gel 4	481.9	0.0	0.0	0.0	0.0
	Mean ± SD	**589.1 ± 239.2**	**1228.5 ± 1020.7***	**292.7 ± 292.7**	**298.3 ± 298.3**	**102.1 ± 102.1**

Table S1 (continuation). Proteins displaying differences in abundance in Sparus aurata liver after 96 h exposure to gold nanoparticles (citrate coated – cAuNPs and polyvinylpyrrolidone coated – PVP-AuNPs), assessed by 2-DE. Values of protein expression are presented as spot density per gel replica and mean spot density of the four gels ± standard error (SD).

		Protein Expression				
Protein Number		**Control**	**7 nm cAuNPs**	**7 nm PVP-AuNPs**	**40 nm cAuNPs**	**40 nm PVP-AuNPs**
21	Gel 1	0.0	171.6	0.0	0.0	312.9
	Gel 2	2029.4	662.4	0.0	0.0	0.0
	Gel 3	0.0	0.0	0.0	0.0	0.0
	Gel 4	181.7	107.7	0.0	0.0	0.0
	Mean ± SD	**552.8 ± 494.1**	**235.4 ± 146.7***	**0.0 ± 0.0***	**0.0 ± 0.0***	**78.2 ± 78.2***
22	Gel 1	819.9	496.8	993.3	0.0	473.0
	Gel 2	2450.3	0.0	0.0	0.0	0.0
	Gel 3	0.0	0.0	342.4	437.9	226.5
	Gel 4	421.0	1142.1	0.0	0.0	0.0
	Mean ± SD	**922.8 ± 536.0**	**409.7 ± 541.5***	**333.9 ± 270.8**	**109.5 ± 109.5**	**174.9 ± 112.8***
23	Gel 1	0.0	826.1	2565.7	0.0	0.0
	Gel 2	0.0	0.0	0.0	2732.3	1941.5
	Gel 3	3981.9	2063.3	0.0	0.0	1453.2
	Gel 4	0.0	0.0	0.0	889.6	552.7
	Mean ± SD	**995.5 ± 995.5**	**722.4 ± 487.6**	**641.4 ± 641.4**	**905.5 ± 644.0**	**986.8 ± 437.0***
24	Gel 1	0.0	236.1	631.9	924.5	0.0
	Gel 2	223.0	1683.0	0.0	0.0	0.0
	Gel 3	0.0	417.4	0.0	0.0	0.0
	Gel 4	177.2	1437.0	0.0	0.0	247.0
	Mean ± SD	**100.1 ± 58.5**	**943.4 ± 361.4***	**158.0 ± 158.0**	**231.1 ± 231.1**	**61.8 ± 61.8**

Table S1 (continuation). Proteins displaying differences in abundance in Sparus aurata liver after 96 h exposure to gold nanoparticles (citrate coated – cAuNPs and polyvinylpyrrolidone coated – PVP-AuNPs), assessed by 2-DE. Values of protein expression are presented as spot density per gel replica and mean spot density of the four gels ± standard error (SD).

		Protein Expression				
Protein Number		**Control**	**7 nm cAuNPs**	**7 nm PVP-AuNPs**	**40 nm cAuNPs**	**40 nm PVP-AuNPs**
25	Gel 1	3250.8	63.3	0.0	4008.4	2844.4
	Gel 2	3909.9	0.0	3892.8	3822.8	912.3
	Gel 3	1269.8	0.0	0.0	0.0	0.0
	Gel 4	0.0	0.0	0.0	0.0	0.0
	Mean ± SD	**2107.6 ± 899.0**	**15.8 ± 15.8***	**973.2 ± 973.2**	**1957.8 ± 1131.0**	**939.2 ± 670.5**
26	Gel 1	346.6	644.6	0.0	0.0	0.0
	Gel 2	0.0	0.0	0.0	0.0	0.0
	Gel 3	987.6	865.7	0.0	0.0	0.0
	Gel 4	900.4	0.0	0.0	0.0	0.0
	Mean ± SD	**558.7 ± 234.1**	**377.6 ± 222.6**	**0.0 ± 0.0*#**	**0.0 ± 0.0*#**	**0.0 ± 0.0*#**

Table S2. Matrix assisted laser desorption/ionisation time of flight (MALDI-TOF/TOF) identification of the proteins displaying differences in abundance in *Sparus aurata* liver after 96 h exposure to gold nanoparticles. Proteins identified using the UNIPROT database. Mr – Molecular Weight; MS – Mass Spectrometry; MS/MS – Tandem-Mass Spectrometry.

							Matched Peptides			
Protein Number	**Gene ID**	**Mr (KDa)**	**Protein Name**	**Accession Number**	**Species**	**Protein Score**	**MS**	**MS/MS**	**Ion Score**	**Peptide Sequence**
1	EEF1G	168,763	Elongation factor 1-gamma	A0A0F8C4B3	*Larimichthys crocea*	80	58	0	-	-
2	HSP90	92,772	94 kDa glucose-regulated protein	M9NZ74	*Sparus aurata*	200	34	4	58 76 32 22	R.GLFDEYGSK.K K.SILFVPTSAPR.G K.GVVDSDDLPLNVSR.E K.EVEEDEYTAFYK.T
3	PCK2	69,778	Phosphoenolpyruvate carboxykinase 2 (mitochondrial)	F1R9Y5	*Danio rerio*	73	22	1	51	K.IFHVNWFR.K
4	GKUP	56,095	Glucuronokinase with putative uridyl pyrophosphorylase	A0A0R4IGN7	*Danio rerio*	86	34	0	-	-
5	ATP5B	55,130	ATP synthase subunit beta	A8WGC6	*Danio rerio*	396	30	6	31 70 27 56 93 49	R.IPVGPETLGR.I K.AHGGYSVFAGVGER.T R.VALTGLTVAEYFR.D R.LVLEVAQHLGENTVR.T R.DQEGQDVLLFIDNIFR.F R.AIAELGIYPAVDPLDSTSR.I

Table S2 (continuation). MALDI-TOF/TOF identification of the proteins displaying differences in abundance in *Sparus aurata* liver after 96 h exposure to gold nanoparticles. Proteins identified using the UNIPROT database.

							Matched Peptides			
Protein Number	**Gene ID**	**Mr (KDa)**	**Protein Name**	**Accession Number**	**Species**	**Protein Score**	**MS**	**MS/MS**	**Ion Score**	**Peptide Sequence**
6	SHMT2	54,439	Mitochondrial serine hydroxymethyltransferase	A9LDD9	*Danio rerio*	95	17	3	26 17 25	K.YSEGYPGKR.Y K.LIIAGTSAYAR.L R.GLELIASENFCSR.A
7	CPA	53,490	Carboxypeptidase	G3NFY9	*Gasterosteus aculeatus*	144	7	2	133 1	K.NELFLTGESYGGIYIPTLAER.V R.LFPEFSKNELFLTGESYGGIYIPTLAER.V
8	PC	52,015	Pyruvate carboxylase b	B0S5R6	*Danio rerio*	71	19	1	41	K.YGNVIHLYER.D
9	SELENBP1	50,983	Selenium-binding protein 1	Q6PHD9	*Danio rerio*	138	11	3	28 46 49	R.LILPSLISSR.I R.EEIVYLPCIYR.N R.FLYFSNWLHGDIR.Q
10	TUBB2B	49,717	Tubulin beta chain	Q32PU7	*Danio rerio*	124	21	4	21 23 42 6	R.FPGQLNADLR.K R.INVYYNEASGGK.Y K.GHYTEGAELVDSVLDVVR.K R.SGPFGQVFRPDNFVFGQSGAGNNWAK.G
11	TUBB2B	49,717	Tubulin beta chain	Q32PU7	*Danio rerio*	169	20	2	69 56	R.FPGQLNADLR.K K.GHYTEGAELVDSVLDVVR.K
12	CYTH1	48,704	Cytohesin-1	A0A146RY54	*Fundulus heteroclitus*	64	28	0	-	-

Table S2 (continuation). MALDI-TOF/TOF identification of the proteins displaying differences in abundance in *Sparus aurata* liver after 96 h exposure to gold nanoparticles. Proteins identified using the UNIPROT database.

							Matched Peptides			
Protein Number	**Gene ID**	**Mr (KDa)**	**Protein Name**	**Accession Number**	**Species**	**Protein Score**	**MS**	**MS/MS**	**Ion Score**	**Peptide Sequence**
13	CALR	48,640	Calreticulin	F1Q8W8	*Danio rerio*	110	12	1	94	K.YDSIGVIGLDLWQVK.S
14	BHMT	44,082	Betaine--homocysteine S-methyltransferase 1	F1QU55	*Danio rerio*	156	16	2	106 23	R.LNAGEVVIGDGGFVFALEK.R R.AGSNVMQTFTFYASDDKLENR.G
15	ACTBA	41,767	Actin, cytoplasmic 1	Q7ZVI7	*Danio rerio*	528	22	7	36 56 33 58 104 105 61	K.AGFAGDDAPR.A R.GYSFTTTAER.E R.AVFPSIVGRPR.H K.IWHHTFYNELR.V K.SYELPDGQVITIGNER.F R.VAPEEHPVLLTEAPLNPK.A K.DLYANTVLSGGTTMYPGIADR.M
16	ACTBA	41,767	Actin, cytoplasmic 1	Q7ZVI7	*Danio rerio*	222	19	4	30 20 74 59	R.GYSFTTTAER.E K.IWHHTFYNELR.V K.SYELPDGQVITIGNER.F R.VAPEEHPVLLTEAPLNPK.A
17	ACTBA	41,767	Actin, cytoplasmic 1	Q7ZVI7	*Danio rerio*	309	15	5	6 59 112 94 9	R.GYSFTTTAER.E K.IWHHTFYNELR.V K.SYELPDGQVITIGNER.F R.VAPEEHPVLLTEAPLNPK.A K.DLYANTVLSGGTTMYPGIADR.M
18	ACTBA	41,767	Actin, cytoplasmic 1	Q7ZVI7	*Danio rerio*	282	24	4	36 94 48 18	K.IWHHTFYNELR.V K.SYELPDGQVITIGNER.F R.VAPEEHPVLLTEAPLNPK.A K.DLYANTVLSGGTTMYPGIADR.M

Table S2 (continuation). MALDI-TOF/TOF identification of the proteins displaying differences in abundance in *Sparus aurata* liver after 96 h exposure to gold nanoparticles. Proteins identified using the UNIPROT database.

							Matched Peptides			
Protein Number	**Gene ID**	**Mr (KDa)**	**Protein Name**	**Accession Number**	**Species**	**Protein Score**	**MS**	**MS/MS**	**Ion Score**	**Peptide Sequence**
19	ACTBB	41,753	Actin, cytoplasmic 2	Q7ZVF9	*Danio rerio*	74	16	1	47	K.SYELPDGQVITIGNER.F
20	ACTBB	41,753	Actin, cytoplasmic 2	Q7ZVF9	*Danio rerio*	84	22	1	52	K.SYELPDGQVITIGNER.F
21	ACTBB	41,753	Actin, cytoplasmic 2	Q7ZVF9	*Danio rerio*	84	18	2	9 98	K.IWHHTFYNELR.V K.SYELPDGQVITIGNER.F
22	FAH	38,754	Fumarylacetoacetate hydrolase (Fumarylacetoacetase)	Q803S0	*Danio rerio*	165	14	3	34 33 87	R.LPVGYHGR.A R.DHATNVGIMFR.G R.DIQAWEYVPLGPFLGK.N
23	HPCA	22,317	Hippocalcin	I3JLG1	*Oreochromis niloticus*	64	16	1	5	R.QMDLNNDGKLSLEEFIKGAK.S
24	FGF1B	17,855	Fibroblast growth factor	A7YT71	*Danio rerio*	64	16	0	-	-
25	PPIA	17,732	Peptidyl-prolyl cis-trans isomerase	Q4S1X7	*Tetraodon nigroviridis*	230	12	2	69 141	K.FADENFQLK.H K.HVVFGKVVEGIDVVK.A
26		5,067	Uncharacterised protein	A0A0E9WUZ5	*Anguilla anguilla*	62	10	0	-	-